Oxide Charge And Sodium Mobility In Gamma-irradiated Silicon-dioxide Films.

OXIDE CHARGE AND SODIUM MOBILITY IN GAMMA-IRRADIATED SILICON DIOXIDE FILMS

by

Frederick Everett Witherell, Jr.

A Dissertation
Presented to the Graduate Committee
of Lehigh University
in Candidacy for the Degree of
Doctor of Philosophy
in
Chemical Engineering

Lehigh University

1974

Approved and recommended for acceptance as a dissertation in partial fulfillment of the requirements for the degree of Doctor of Philosophy.

8/28/74

Frederick M. Forkes
Professor in Charge

Accepted 8/28/74

Special committee directing the doctoral work of Mr. Frederick Everett Witherell, Jr.

Frederick M. Forkes
Chairman

Colin S. Jones

Gary Poehlein

C. W. Chung

James E. Sturm

ACKNOWLEDGEMENTS

The author wishes to acknowledge the encouragement and interest, not to mention patience, of his dissertation advisor, Professor Frederick M. Fowkes. The advice of the author's special committee is also acknowledged. The author is grateful to Mr. James G. Flood, who developed the fluorometric analysis technique. The advice of Mr. Thomas E. Burgess and Miss Helen M. Donega of Burgess Analytical in the development of the radiotracer and fluorometric techniques is sincerely appreciated. The Ion Microprobe analyses were performed by Mr. Richard Hunsberger of Bell Telephone Laboratories, Reading, Pennsylvania. The assistance of Dr. Dennis W. Hess, presently of Fairchild Research and Development, in mastering a number of experimental techniques, and for countless helpful discussions, is gratefully acknowledged.

The financial support of the National Science Foundation and the Defense Nuclear Agency is gratefully acknowledged.

The author is especially grateful to his parents for their continued encouragement, and to his wife, Marilyn, for her patience and understanding, without which the completion of this dissertation would have been impossible.

TABLE OF CONTENTS

LIST OF TABLES

LIST OF FIGURES

ABSTRACT

A study has been made of the effects of gamma-irradiation and aluminum doping on sodium mobility in thermally grown silicon dioxide films on silicon. Aluminum can be diffused through 2000 Å silicon dioxide films in 30 minutes at 500°C. The aluminum content in the films near the $Si-SiO_2$ interface increases with increasing diffusion time. Moderate aluminum doping causes a decrease in interfacial sodium concentration, compared with undoped films. However, as the interfacial aluminum content increases with continued aluminum diffusion, interfacial sodium concentration increases again. These results suggest that aluminum is able to sequester sodium to those regions of the film where aluminum content is highest.

Exposure of silicon dioxide films to gamma radiation results in positive oxide charge build-up, as measured by flat-band voltage shifts in the capacitance-voltage characteristics of MOS capacitors. The interfacial sodium concentration does not increase significantly during this treatment. Irradiation followed by positive bias-temperature stress results in large increases in the interfacial sodium concentration for undoped and heavily aluminum doped oxides, but not for moderately aluminum-doped oxides.

These results are consistent with a model in which sodium can be extracted from the $Si-SiO_2$ interface by substitutional aluminum impurities, resulting in reduced sodium mobility during irradiation and bias-temperature stress.

I. INTRODUCTION

The advent of the planar silicon semiconductor technology, in which the silicon surface is stabilized by an insulating film, has resulted in considerable miniaturization of complicated electronic circuitry. While a number of technologies have benefitted from this development, perhaps the most important applications of miniaturized integrated circuitry have been in the space industry. The development of compact, lightweight electronic computers, guidance systems, and other sophisticated electronic components would have been impossible without the planar technology.

However, the use of solid-state electronic devices in space applications led to the discovery that high-energy radiation caused perturbations in device performance, and, eventually, device failure. In addition, certain device fabrication steps, such as electron-beam metallization and ion-implantation, expose the devices to radiation doses of sufficient magnitude to cause variations in device characteristics. Although high-energy radiation can cause considerable damage in silicon, the most serious form of radiation damage in planar semiconductor devices results from a build-up of charge in the insulating oxide film which covers the silicon substrate.

Most semiconductor devices are modifications of a basic structure consisting of a silicon wafer covered with a thin (1,000-10,000 Å) film of silicon dioxide. Deposition of a metal electrode (usually aluminum, and known as a gate electrode) over the oxide

results in the so-called MOS (metal-oxide-silicon) capacitor illustrated in Fig. 1. Although actual commercial devices may be considerably more complicated than this, the MOS capacitor is a convenient structure for the illustration and investigation of many semiconductor device properties.

The physics of semiconductor devices has been the object of intense investigation for many years, and several excellent texts on the subject are available (1,2). An understanding of basic device physics will be assumed in the ensuing discussions.

The properties of MOS devices are controlled primarily by phenomena occurring near the Si-SiO_2 interface. Silicon dioxide films in MOS devices generally are imperfect insulators, due principally to the presence of impurity ions (mostly sodium) in concentrations of parts per billion. Under normal device operation conditions the sodium tends to be immobile. Under certain conditions, however, such as elevated temperatures combined with high electric fields, the sodium becomes mobile and drifts through the oxide as an interstitial cation. If the field is directed so that the ions drift toward the Si-SiO_2 interface and build up there, the properties of the interface, and, therefore, those of the device, will be affected. The resulting positive charge accumulation can be observed as a shift in the capacitance-voltage characteristics of the capacitor to more negative voltages, as illustrated in Fig. 2. In commercial MOS transistors, the charge results in shifts in the threshold voltage.

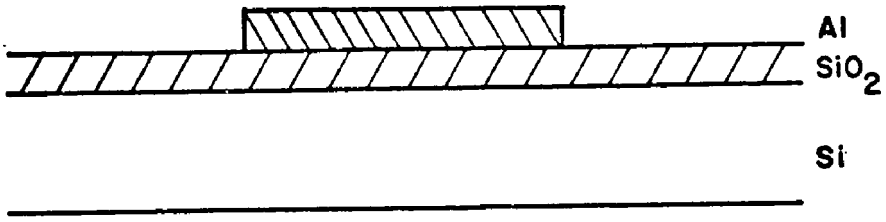

Fig. 1 Metal-oxide-silicon (MOS) capacitor

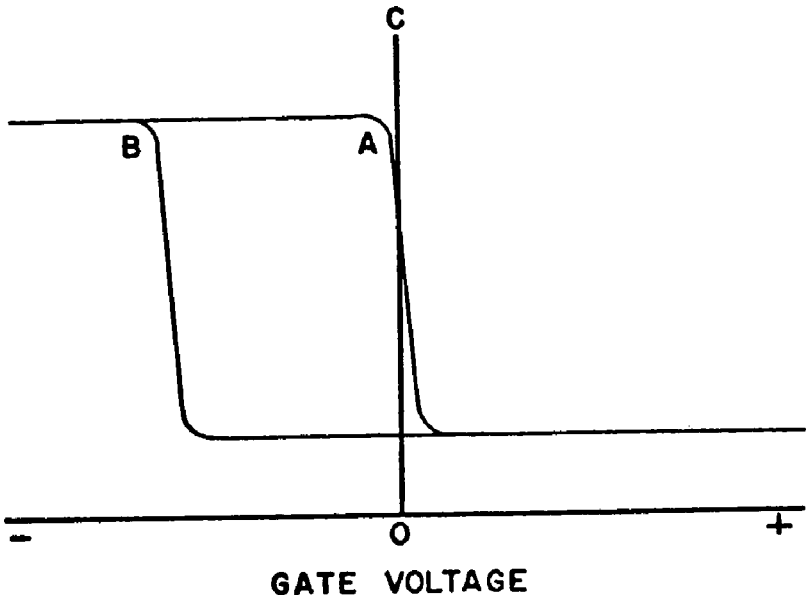

Fig. 2 Capacitance-voltage characteristic of MOS capacitors; A: ideal capacitor; B: capacitor with positive charge present in the oxide; p-type silicon.

Although it is commonly accepted that sodium ions are the most common source of oxide charge, other sources are possible. Evidence will be presented which suggests that ionized oxygen vacancies may be equally important.

If an MOS device is fabricated using p-type silicon (i.e., the majority current carriers in the silicon are holes), a positive voltage applied to the gate electrode will cause the positively-charged holes in the silicon surface region to drift away from the Si-SiO_2 interface. At the same time, electrons in the silicon will be attracted toward the interface. If the applied voltage is of sufficient magnitude, the concentration of electrons in the silicon surface region will be greater than that of holes, and a channel of n-type silicon will be formed, as illustrated in Fig. 3. Exposure of such an n-channel device to radiation of energy greater than the silicon dioxide band-gap (8.6 eV) leads to accumulation of positive charge in the oxide. The source of this charge has not been identified, although it is commonly assumed to be sodium ions and/or holes. Trapping of radiation-generated holes at oxygen vacancies near the interface is also likely to contribute to the oxide charge. Although several methods exist for analysis of the sodium content of silicon dioxide films, none of them has been applied to the problem of irradiated films in order to determine whether sodium is mobile under these conditions.

A number of empirical methods have been developed to reduce oxide charge build-up during irradiation, including pre-

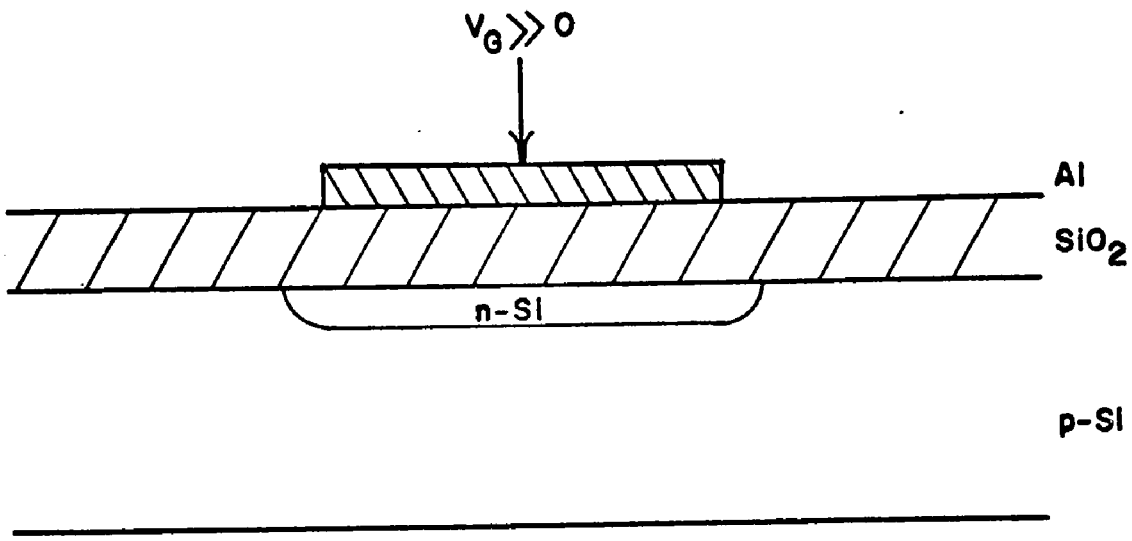

Fig. 3 Formation of n-channel in p-type silicon by application of positive gate voltage.

paration of "clean," i.e., impurity-free, oxide films; replacement of silicon dioxide with another insulator, such as aluminum oxide, silicon nitride, or silicon oxynitride; or doping of the oxide with metallic impurities, such as aluminum or chromium, which in some way neutralize the charge. Of these, the latter method has received the most attention, and appears to be the most promising. However, the role played by the metal impurity ions is not well understood. In particular, although work on bulk silicon dioxide indicates a possible interaction between aluminum and sodium, such an interaction in thin films has not been systematically investigated.

We have undertaken a study of several aspects of radiation effects in silicon dioxide films. First, we have investigated the relationship between oxide charge and sodium mobility in unirradiated films, and in films irradiated with 1.25 MeV gamma rays. Second, we have examined thermal diffusion as a method for introducing aluminum into silicon dioxide films. Third, we have investigated the role of aluminum in reducing oxide charge and decreasing sodium mobility in unirradiated and gamma-irradiated films.

2. RADIATION STUDIES ON BULK AND THIN FILM SILICON DIOXIDE

A. Radiation Studies on Quartz and Fused Silica

Radiation effects in bulk crystalline quartz, fused silica, and silicate glasses have been extensively studied over the past twenty years, and the early work has been reviewed (3). Ionizing radiation produces defect centers which are both optically and magnetically active, and many investigators have attempted to correlate these centers with certain impurities, particularly aluminum and alkali. While the exact structure of radiation-related defects is not known, several useful models have been suggested.

The appearance of visible coloration, optical absorption, and paramagnetic resonance signals in natural "smoky" and X-irradiated synthetic quartz was studied by Ditchburn, et al. (4) and by Griffiths, Owen and Ward (5). The presence of a paramagnetic signal resulting from the ^{27}Al nucleus led O'Brien (6) to suggest a model for the active center which involved aluminum in a substitutional position for silicon in the lattice. Since aluminum is trivalent, it must capture an electron in order to form the required four bonds to oxygen, and thus it bears a negative charge. An interstitial hydrogen or alkali ion was assumed to be present for charge compensation. O'Brien postulated that upon irradiation the aluminum center lost an electron along with the charge-compensating ion.

Mitchell and Paige (7) obtained good correlation between the optical absorption intensity of X-irradiated quartz samples and their aluminum content. However, the coloration is believed to be related to the charge-compensating alkali ion, rather than the aluminum center itself. Lell (8) found that samples containing only hydrogen as the charge compensator were highly resistant to coloration upon X-irradiation. When alkali ions were present, the extent of coloration was dependent upon the particular alkali ion, with lithium producing greater coloration than sodium, which in turn was more effective than potassium.

Important papers by Lineweaver and Sigel have siggested that hydrogen and alkali ions can also be localized as charge compensators for non-bridging oxygen atoms, i.e., oxygen atoms which are bonded to only one silicon atom. While the existence of such species has not been proved, it is apparent that traps other than the aluminum center do exist.

Lineweaver (9) observed coloration and the evolution of oxygen gas upon electron bombardment of alkali silicate glasses. He proposed a mechanism in which alkali ions associated with non-bridging oxygens are freed due to the capture by the oxygens of radiation-generated holes. The removal of the stabilizing influence of alkali ions allows neighboring non-bridging oxygens to react, restoring the silicon-oxygen-silicon bridges and releasing oxygen:

$$\equiv Si\text{-}O^{-}\,h^{\cdot}\;\; h^{\cdot}\,{}^{-}O\text{-}Si\equiv \rightarrow \equiv Si\text{-}O\text{-}Si\equiv + 1/2\; O_2 \qquad (1)$$

Sigel (10)studied the interrelationships between aluminum, sodium and non-bridging oxygens in an unirradiated fused silica.

He found that introduction of alkali ions into fused silica shifted the ultraviolet absorption edge to longer wavelengths, the extent of the shift being dependent upon alkali content. Subsequent addition of aluminum to the silica brought the absorption edge back near its original value. These results were interpreted to indicate that alkali ions introduced non-bridging oxygens into the silica, shifting the absorption edge. Aluminum doping tied up the alkali, thus reducing the non-bridging oxygen content.

As previously mentioned, unequivocal correlations between observed radiation effects and proposed models for the centers responsible for such effects are often difficult to develop. For example, a direct correspondence between aluminum content in quartz and radiation-induced optical absorption intensity is not always observed (11). Also, the intensity of the aluminum center electron paramagnetic resonance spectrum in irradiated quartz is quite temperature dependent (12,13), while the optical spectrum remains essentially unaltered between 77 and 300°K (13,14). Lineweaver's results have been questioned by Jones (15), who has found no change in the intensity of SiOH (H-compensated non-bridging oxygen) infrared absorption bands upon X-irradiation of quartz.

In spite of these difficulties, the results presented above lend themselves to the suggestion of mechanisms for the observed radiation effects. Fig. 4 illustrates two possible suggestions.

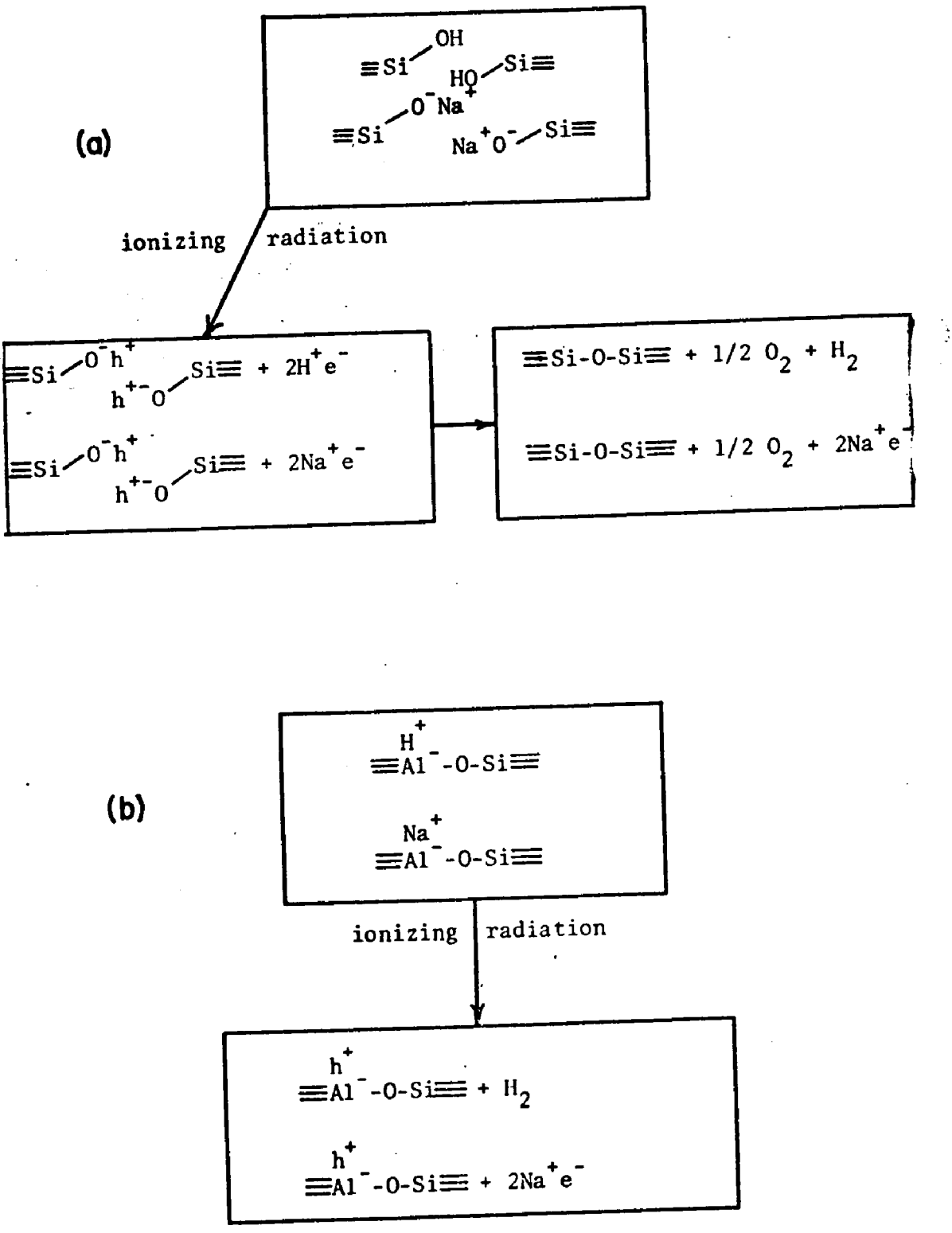

Figure 4. Suggested radiation-induced defect mechanisms in SiO_2. (a) Non-bridging oxygen; (b) Substitutional aluminum

The introduction of hydrogen or alkali ions into the SiO_2 lattice may result in the formation of non-bridging oxygen sites in the form of hydroxyls or oxygen-alkali ion pairs. If radiation-generated holes are trapped by such sites the cation can be released, and would be expected to be an electron trap. The alkali could remain in this form, and produce the coloration characteristic of irradiated quartz. However, hydrogen ions with trapped electrons (i.e., hydrogen atoms) might well combine to form hydrogen gas. The non-bridging oxygen sites can then react, reforming the Si-O-Si bridge by eq. 1, and releasing oxygen gas, as observed by Lineweaver (9). Such a mechanism is illustrated in Fig. 4(a).

Fig. 4(b) illustrates a possible mechanism for the radiation-induced aluminum center formation. The negatively charged substitutional aluminum is thought to be initially compensated by an alkali ion or proton. Upon irradiation, the alkali ion or proton is displaced by a hole, becoming free to move through the lattice until it stabilizes an electron. Again, the alkali ion plus trapped electron configuration could be stable, while hydrogen atoms can form hydrogen gas. Such a mechamism would explain why hydrogen does not contribute to coloration.

Of particular importance is the observation that the non-bridging oxygen center is not permanent. It reverts to the original Si-O-Si structure. On the other hand, the aluminum center is a permanent hole trap, as illustrated in Fig. 4(b).

B. Thin Film Silicon Dioxide

1. Silicon-Silicon Dioxide Interface System

The radiation effects of interest in most thin film studies occur at or near the silicon-silicon dioxide interface. Certain aspects of this interface were considered briefly in Ch. 1. It was mentioned that silicon dioxide is an imperfect insulator due to the presence of various charged species. Charges in the oxide, and particularly those near the $Si-SiO_2$ interface, induce a space charge of opposite sign in the surface region of the silicon due to attraction or repulsion of charge carriers. The formation of such a space-charge region in p-type silicon is illustrated in Fig. 5. If no oxide charge is present, as in Fig. 5(a), charge neutrality in the silicon surface region is maintained due to the presence of equal numbers of negative acceptor impurities and positive holes. In Fig. 5(b), positive charge has been introduced into the oxide. Holes in the silicon surface region are repelled by this charge, and the surface is depleted of majority carriers, creating a negative space-charge region due to ionized acceptor atoms.

Application of a negative voltage to the gate electrode of the MOS capacitor will have the opposite effect of attracting holes from the bulk silicon toward the surface, and into the space-charge region. If the negative voltage is of sufficient magnitude, enough holes will be returned to the space-charge region to neutralize the charge. Such a condition, in which no net charge exists at the $Si-SiO_2$ interface, is called the flat-band condition, since

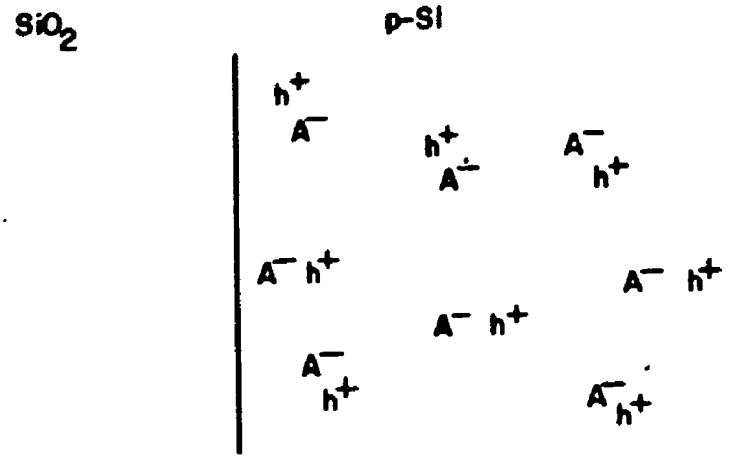

(a) no oxide charge

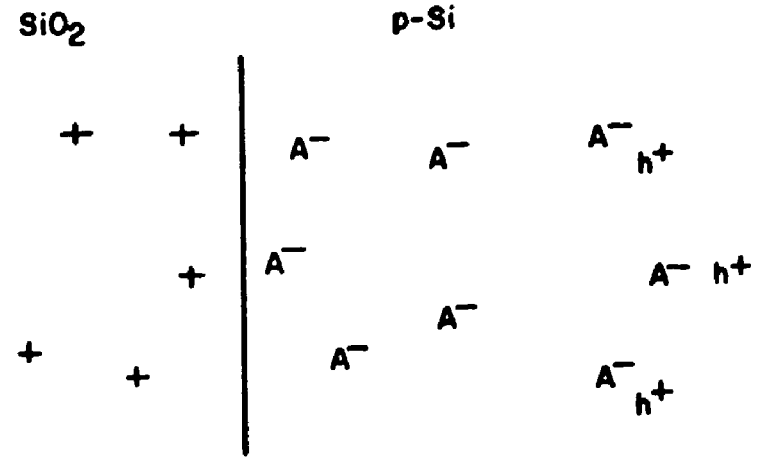

(b) positive oxide charge

Fig. 5 Formation of space-charge region in p-type silicon due to the presence of positive oxide charge.

the silicon energy bands, which will bend in the presence of a space-charge, are flat when no space-charge is present. The voltage required to achieve this condition is the flat-band voltage, V_{FB}. If there is no oxide charge, as in Fig. 5(a), V_{FB} equals zero. A negative flat-band voltage indicates the presence of positive oxide charge, while a positive V_{FB} means that negative charge exists in the oxide.

The amount of charge present in the oxide can be calculated with the help of the capacitance-voltage (C-V) characteristic of the MOS capacitor. As stated in Ch. 1, oxide charge causes a shift in the C-V curve. The value of the capacitance at flat-band conditions, C_{FB}, can be determined from the oxide capacitance, C_{ox}, and the silicon donor atom concentration (16). V_{FB} is then measured as indicated in Fig. 6, curve B, and the amount of oxide charge per unit area, Q_{ox}/q, can be calculated (1,2):

$$\frac{Q_{ox}}{q} = - \frac{C_{ox} V_{FB}}{Aq} \qquad (2)$$

where q is the electronic charge, and A is the gate electrode area.

Oxide charge can be either fixed or mobile. Fixed charge is immobile under all conditions. Its origin is uncertain, although recent work by Fowkes and Hess (17) indicates that fixed charge may result from partially ionized oxygen vacancies near the $Si-SiO_2$ interface.

If the oxide charge is due to mobile ionic impurities, the extent of their mobility may be studied by application of a

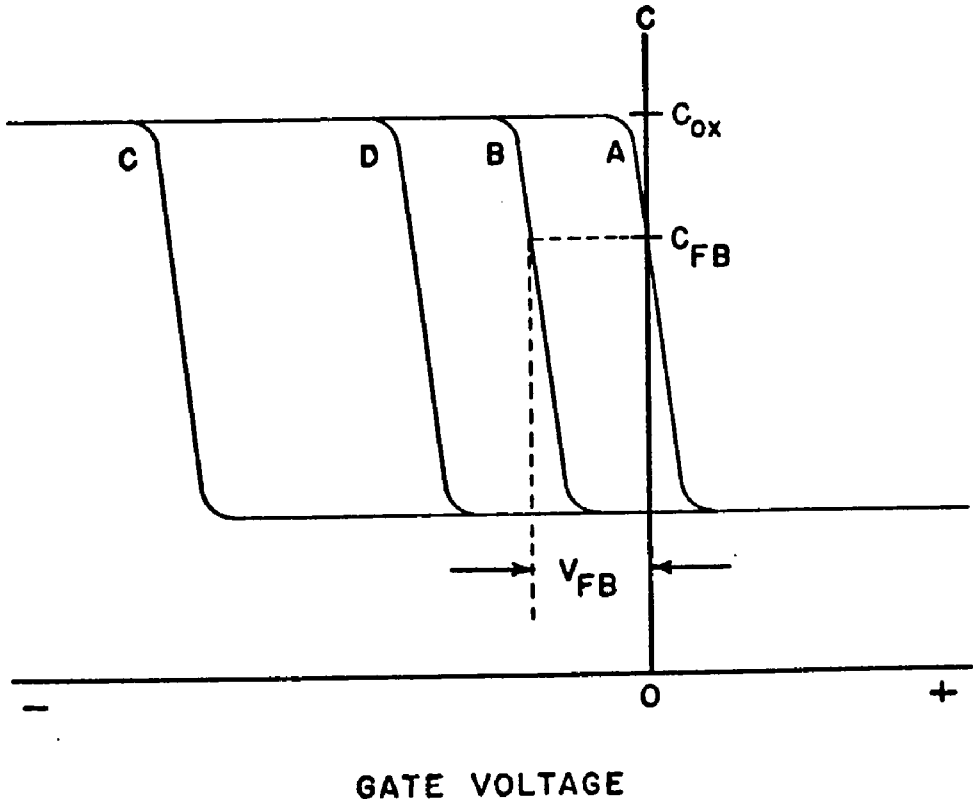

Fig. 6 Effect of positive oxide charge on capacitance-voltage characteristics of MOS capacitor. A: no oxide charge. B: effect of oxide charge; C: effect of increase in charge due to positive bias-temperature stress; D: partial reversal due to negative bias-temperature stress.

gate bias at elevated temperatures (bias-temperature stress). Application of a positive bias will move mobile positive charges in the oxide toward the Si-SiO_2 interface, where their effect upon the silicon space-charge region will be stronger. This drift will result in an increase in V_{FB}, as indicated in Fig. 6, curve C. Subsequent application of a negative bias results in partial reversal, as shown in curve D.

2. Metallic Diffusion in Silicon Dioxide Films

The most common impurity present in silicon dioxide films is sodium, which occurs as interstitial cations. A portion of these ions is trapped in the oxide, probably at non-bridging oxygen sites (18) as illustrated in Fig. 4(a). The sodium generally assumes a U-shaped concentration profile across the oxide, as illustrated in Fig. 7, with surface and interface concentrations several orders of magnitude higher than that in the bulk. The profiles in the surface and interface regions can be described by the Poisson-Boltzman distribution (18,19). This point will be discussed in more detail in Ch. 3.

Most sodium is not mobile at room temperature, even under the influence of strong electric fields. However, at elevated temperatures much of the sodium is observed to drift under the influence of even moderate fields. Such drift will alter the sodium distribution and the oxide charge.

Aluminum contamination is also common in silicon dioxide films, although its mobility has received less attention than that

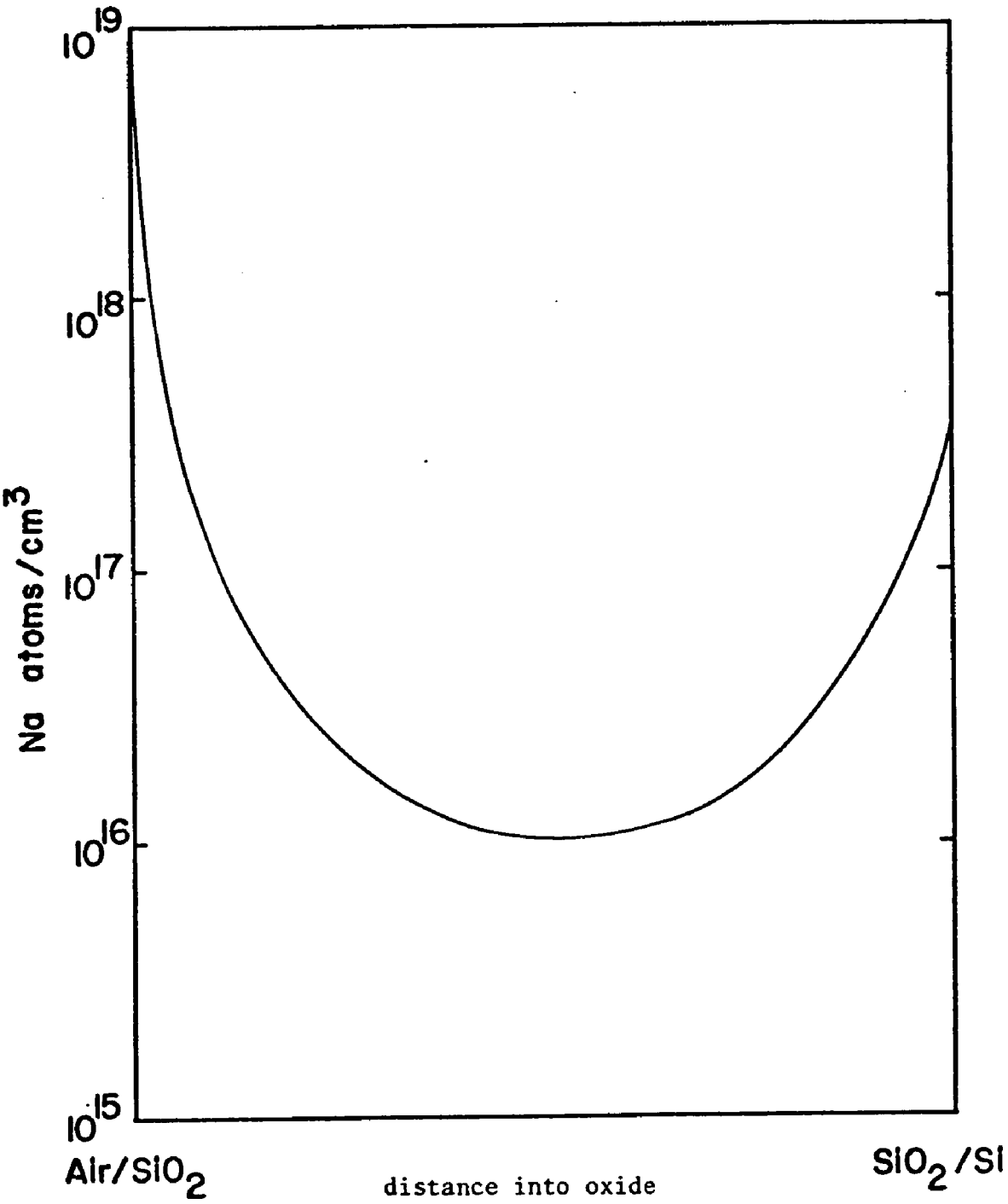

Fig. 7 Typical sodium distribution in thermally grown SiO_2 film.

of sodium. Fowkes, Burgess, and Hutchins (20) found that aluminum diffused into silicon dioxide films when aluminum-covered films were heated at 500°C. The diffusion induced phase separation and dendritic growth of an oxide phase containing three silicon atoms per aluminum atom, as determined by electron microprobe. Chou and Eldridge (21) determined that 500°C annealing of aluminum electrodes on 1000 Å silicon dioxide films resulted in a reaction between aluminum and silicon dioxide, forming an aluminum oxide-silicon oxide phase. This phase penetrated through the oxide within thirty minutes.

Donega, Burgess and Baker (22) diffused aluminum into oxide films for twenty minutes at 530°C in nitrogen. The films were then etched in steps, and the etch solutions analyzed for aluminum by a colorimetric technique. The profile obtained was very similar to the U-shaped profiles for sodium (see Fig. 7), although the concentrations were several orders of magnitude higher.

C. Radiation Effects in Thin Silicon Dioxide Films

The effects of ionizing radiation on MOS devices have been reviewed by Mitchell and Wilson (23). The principal effect is a build-up of positive charge in the oxide. For positive gate bias during irradiation, Snow, Grove and Fitzgerald (24) found that the positive charge build-up saturated with radiation dose, and that for a constant dose, the charge increased with gate bias. In addition, the radiation-induced charge was located within several hundred

angstroms of the $Si-SiO_2$ interface.

Introduction of aluminum into the oxide has generally improved the stability of oxide films during positive gate bias irradiation. During the thermal growth of silicon dioxide films in dry oxygen, Revesz, Zaininger and Evans (25) introduced aluminum into their oxidizing ambient. They found that oxides grown in such a manner were less susceptible to positive charge build-up than were oxides grown without aluminum. Similar results were obtained by Peel and Kinoshita (26) after thermal diffusion of aluminum (480°C, thirty minutes) into their oxides. In neither of these studies, however, were impurity concentration profiles determined.

Hughes, Baxter and Phillips have examined aluminum concentration profiles in silicon dioxide films, after aluminum electrode annealing, using an ion microprobe. The aluminum content of the films was approximately an order of magnitude higher after a twenty minute anneal at 500°C than after a 300°C anneal. The oxides annealed at 500°C were also considerably more resistant to γ-radiation-induced charge build-up. Although the aluminum concentration profiles clearly showed diffusion all the way to the $Si-SiO_2$ interface, there was no increase in aluminum content near the interface, as had been observed by Donega, et al. (22). This may be due to the lower diffusion temperature employed. Also, the ion microprobe employs ion sputtering to etch the sample. Such a technique may not etch as uniformly as does chemical etching.

These same investigators also studied aluminum ion implantation as a method for controlling radiation-induced oxide charge. The depth of penetration of the ions was controlled by varying their energies. It was determined that the radiation resistance of the oxide films was increased by shallow and moderate depth implantations. However, when the ions were implanted deep into the oxides, the devices were less resistant to charge build-up than unimplanted devices.

Although the technology involved in controlling radiation effects has been extensively studied, the nature of the radiation-induced positive charge, and the contribution of sodium and other impurities to that charge, is still unclear. Hughes (27) has likened the effects of sodium in thin films to those of sodium in bulk samples, as previously discussed. Thus, sodium can act as a network-modifier, creating non-bridging oxygen sites. Upon irradiation, holes can be trapped at these sites, displacing the sodium cations. It is this sodium which can then move to the interface, resulting in the observed positive charge. Aluminum at substitutional positions in the lattice can trap additional sodium or holes, forming neutral pairs, as it is postulated to do in bulk silica and quartz

Such a theory has not been universally accepted, however. Gwyn (28) has postulated a broken bond mechanism which does not rely on impurities as the charge source. The need for a careful investi-

gation involving analytical determination of aluminum and sodium concentrations and mobilities in irradiated silicon dioxide films is apparent.

3. EXPERIMENTAL DETAILS

A. Silicon Oxidations

Silicon wafers were obtained from Semiconductor Processing Company, Hingham, Massachusetts. They were p-type wafers, boron-doped, 10-40 ohm-cm resistivity, <100> surface orientation.

The wafers were degreased by heating successively for several minutes in trichloroethylene, acetone, and methanol. They were then rinsed in deionized water, and heated in a mixture of five parts deionized water, one part hydrogen peroxide, and one part ammonium hydroxide, by volume. After rinsing in deionized water, the wafers were heated in a mixture of five parts deionized water, one part hydrogen peroxide, and one part hydrochloric acid, by volume. After a subsequent deionized water rinse, the wafers were etched in 5% hydrofluoric acid, rinsed in deionized water, and heated in deionized water. The wafers were then oxidized to several hundred angstroms thickness to remove surface damage. The oxidized wafers were then etched in 5% hydrofluoric acid, rinsed in deionized water, heated in the peroxide solutions as described above, rinsed in deionized water, etched again in 5% hydrofluoric acid, rinsed in deionized water, and heated in deionized water. The wafers were then transferred from the final deionized water rinse directly to the furnace for oxidation.

The oxidations were carried out in a resistance-heated Lindberg three-zone furnace containing a fused quartz oxidation tube

(National Scientific Company, Quakertown, Pennsylvania) and an alumina liner (McDanel Refractory Porcelain Company, Beaver Falls, Pennsylvania). The tube was degreased in trichloroethylene and methanol, rinsed in deionized water, etched in 5% hydrofluoric acid, and rinsed again in deionized water, and air-dried, prior to insertion into the liner. The system was then heated to 1075°C for twenty-four hours with wet nitrogen, which had been bubbled through deionized water at 95°C, flowing through it. The tube was recleaned each month with wet nitrogen in this manner. The furnace was run continuously at 910°C with a small flow of nitrogen. Wafers to be oxidized were supported parallel to the gas flow in a slotted quartz boat which had been previously cleaned with trichlorethylene and methanol, rinsed in deionized water, etched in 5% hydrofluoric acid, rinsed again in deionized water, and air-dried.

All high purity gases were obtained from Air Products and Chemicals, Inc., Allentown, Pennsylvania. They were dried before use by passing through columns of magnesium perchlorate, drierite (W.A. Hammond Co.), then passed into the furnace. Oxidations were performed in dry oxygen at 1075°C. The O_2 flow rate was approximately 1.4 l/min.

B. Sodium Concentration Profiles

The sodium content of the oxides was determined by doping with ^{22}Na and analyzing with liquid scintillation spectrometry. A measured volume of a calibrated $^{22}NaCl$ solution (ICN Radiochemicals,

Cleveland, Ohio) was placed in a quartz boat, and the water evaporated with a heat lamp. The samples were placed face-down into the boat, which was then placed into a Hoskins type FH305 furnace which had been heated to 500°C. The samples were treated in nitrogen at this temperature for two hours.

The outer aluminum film was removed by etching in 2 ml of a 65°C solution of 25 parts phosphoric acid, 5 parts acetic acid, and 1 part nitric acid. Since this process invariably removes some surface sodium, this etch was then mixed with 10 ml of Insta-gel scintillator solution (Packard Instruments, Downers Grove, Ill.) and the ^{22}Na content determined. This value was added to that of the first SiO_2 etch step to calculate the actual surface ^{22}Na content. The ^{22}Na concentration profile was determined by etching successive layers of the oxide in two milliliters of 5% hydrofluoric acid. The acid etches SiO_2 at a rate of 320 Å/min (see Ch. 4). After each etch the sample was rinsed in two milliliters of deionized water. The etch and rinse solutions were then combined in polyethylene vials, ten milliliters of Insta-gel scintillator solution was added, and the contents shaken. The sample β-emission was then counted in a Packard Tri-Carb Model 3330 Liquid Scintillation Counter using coincidence counting techniques. The net count rate was determined by subtracting a background count, determined using an identical solution without ^{22}Na. Calibration was performed by counting standards, again of identical composition, containing a

known amount of ^{22}Na. A typical profile is shown in Fig. 8(a).

The ^{22}Na profile obtained in this manner can be converted to the total sodium profile if it is assumed that the shape of both profiles is the same, and that no other charged species exist in the oxide. It was stated in Ch. 2 that the sodium profiles at the surface and interface follow the Poisson-Boltzmann distribution. The charge density of the ions, ρ, in units of charges/cm^3, at any point x in the oxide is given by the one-dimensional Poisson equation:

$$\frac{d^2\phi}{dx^2} = -\frac{1}{q}\frac{d^2E}{dx^2} = -\frac{\rho}{\epsilon\epsilon_o} \qquad (3)$$

where ϕ = electrostatic potential

E = ionic potential energy

q = ionic charge (+ e for Na^+, +3e for Al^{+3}, etc.)

x = distance into the oxide from the negatively charged surface

ϵ = oxide dielectric constant

ϵ_o = permittivity of free space

For sodium:

$$\rho = e[Na^+] \qquad (4)$$

where $[Na^+]$ is the sodium concentration, in units of ions/cm^3. The attractive forces between the positively charged sodium ions and the negatively charged surface ions is Coulombic; i.e., it falls off with x^{-2}. Thus, a relatively short distance into the

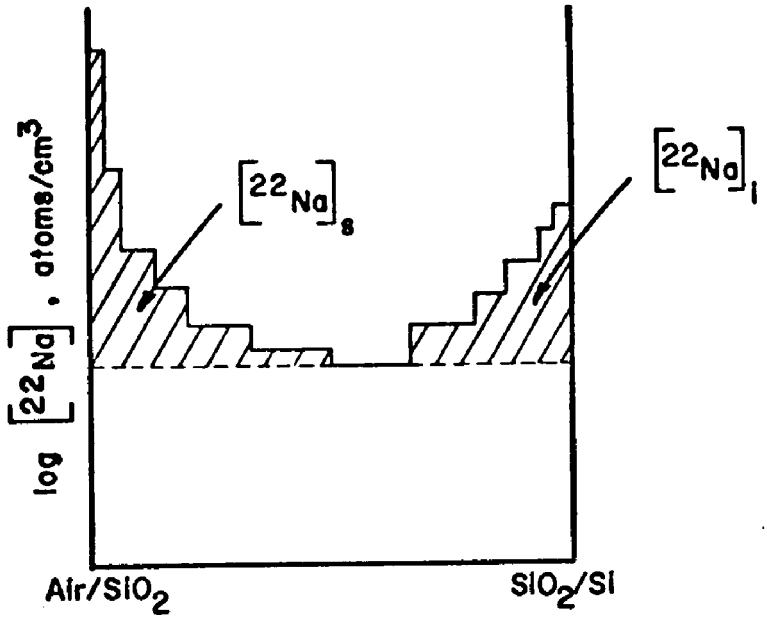

(a) ^{22}Na profile

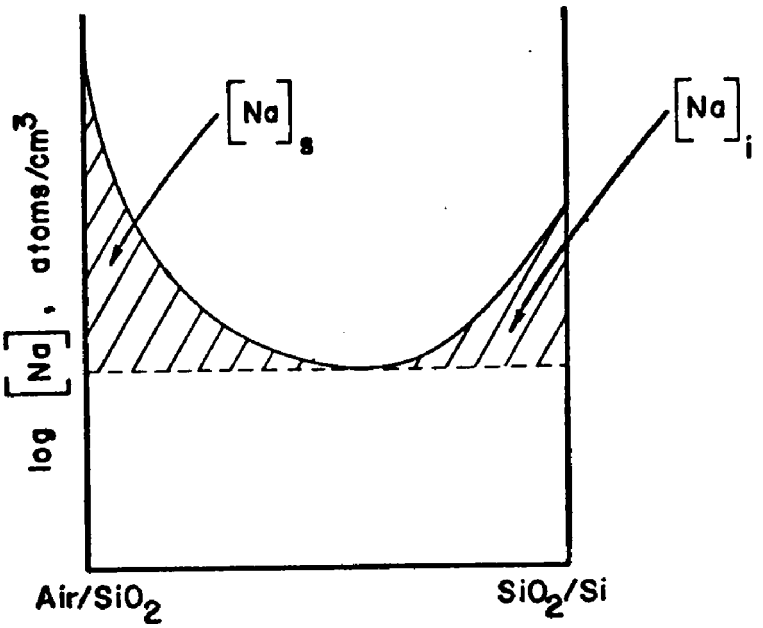

(b) total Na profile

Fig. 8 (a) Experimental ^{22}Na concentration profile.
(b) Total sodium concentration profile.

oxide this interaction becomes negligible. At this point, which we shall call x_o, $[Na^+]=[Na^+]_o$, and dE/dx is equal to zero. Thus:

$$\frac{1}{e}\int_0^{x_o}\frac{d^2E}{dx^2}\,dx = \frac{e}{\varepsilon\varepsilon_o}\int_0^{x_o}[Na^+]dx \qquad (5)$$

or

$$\frac{1}{e}\left.\frac{dE}{dx}\right|_{x=0} = \frac{e}{\varepsilon\varepsilon_o}[Na^+]_s \qquad (6)$$

where $[Na^+]_s$, which has units of ions/cm^2, is the total sodium content per unit area in the surface region, as illustrated in Fig. 8(b).

From Boltzmann statistics the concentration of ions as a function of the potential energy, at a temperature T, can be given:

$$[Na^+] = [Na^+]_o \exp[-(E-E_o)/kT] \qquad (7)$$

Therefore:

$$E-E_o = -2.3\ kT\ \log\frac{[Na^+]}{[Na^+]_o} \qquad (8)$$

and

$$\frac{dE}{dx} = -2.3\ kT\ \frac{d\ \log\ [Na^+]}{dx} \qquad (9)$$

Combining eqs. 6 and 9 yields

$$[Na^+]_s = -\frac{2.3\ kt\varepsilon\varepsilon_o}{e^2}\left.\frac{d\ \log[Na^+]}{dx}\right|_{x=0} \qquad (10)$$

Assuming that the ^{22}Na and total sodium profiles are similar, then

$$\left.\frac{d \log [Na^+]}{dx}\right|_{x=0} = \left.\frac{d \log [^{22}Na^+]}{dx}\right|_{x=0} \qquad (11)$$

and $[Na^+]_s$ can be calculated from the slope of the experimental ^{22}Na profile at the oxide surface. The total ^{22}Na content in the surface region, $[^{22}Na^+]_s$, is also determined from the experimental profile, as shown in Fig. 8(a). Thus, the dilution factor, which is the factor by which the ^{22}Na concentration must be multiplied to obtain the total sodium concentration, is given by $[Na^+]_s/[^{22}Na^+]_s$.

An identical procedure can be followed using the slope and sodium concentrations at the interface, rather than the surface.

C. Aluminum Depositions

Aluminum depositions were performed in a Veeco high vacuum system equipped with a mechanical pump, oil diffusion pump, and liquid nitrogen-cooled cold trap. The aluminum source was a heated tungsten basket filament (Sylvania Emissive Products Co., Exeter, New Hampshire) into which aluminum wire (99.999% pure, Materials Research Corporation, Orangeburg, New York) which had been cleaned with methanol, was placed. Evaporations were performed at 5×10^{-6} torr. The aluminum was evaporated through an aluminum mask in which rectangular holes 0.9 x 1.1 cm had been cut. Electrodes with guard-rings were then prepared by standard photoresist techniques on those samples which were to be analyzed by capacitance-voltage techniques.

Back oxides were removed by etching with 25% hydrofluoric

acid while the front oxide was covered with Apiezon black wax. The wax was removed with trichloroethylene, and the wafers were then rinsed in trichloroethylene, methanol, and deionized water, and blown dry in nitrogen. The entire back of the wafer was then covered with aluminum. Aluminum films were approximately 1500Å thick.

D. Aluminum Diffusions

Aluminum diffusions were performed in a Hoskins type FH305 resistance-heated furnace containing a degreased and etched quartz tube and boat. The oxide surfaces were covered with approximately 1500 Å aluminum films, as in Sec. C, and the wafers were placed horizontally in the boat. The boat was placed in the furnace for the desired time period, at the desired temperature, with dry nitrogen, which was passed through a molecular sieve drying tube, flowing through the furnace tube.

E. Aluminum Concentration Profiles

1. Fluorometric Method

Aluminum ions form a stable complex with the reagent 2',3,4',5,7 pentahydroxyflavone (Morin). At a pH of about 3.0 this complex, Al-$(Morin)_3$, fluoresces at 500 nm when excited by light of wavelength 436 nm (29). The intensity of the fluorescence can be employed to measure the concentration of aluminum ions present in solution.

Application of this technique to profile analysis requires the removal of fluoride ion from the etch solutions; however, since aluminum and fluoride ions also form a stable complex, AlF_6^{-3}, which competes with the Morin complex. This is done by combining the etch solution and 50 µℓ of sulfuric acid in a platinum dish and evaporating to dryness on a hotplate. Another 50 µℓ aliquot of sulfuric acid is added, and the dish is heated until all fuming ceases. The residue is taken up in 3 ml of water and placed into a 10 ml volumetric flask, to which is added 6 ml of 0.1 M potassium acid pthalate buffer and 1 mg of Morin in 1 ml of 95% ethanol. The flask is heated for one minute at 80°C to accelerate complex formation, the solution is transferred to a one centimeter quartz cell, and the fluorescence signal is read at 500 nm with 436 nm light excitation on a Farrand Optical Company fluorometer.

2. Ion Microprobe

The ion microprobe (Cameca Instruments) employs an ion beam to sputter-etch the material to be analyzed. The material removed by the ion beam is analyzed by a mass spectrometer to determine its composition.

For this work an Ar^+ beam was employed to sputter-etch the oxides. The sputtered material was analyzed at seven second intervals, and the data given in ion counts versus sputtering time.

F. Gamma Irradiations

A cobalt-60 gamma-ray source (Picker X-ray Corp., Cleveland, Ohio) was used for sample irradiations. The 1.25 MeV rays, at the dose rate of 10^6 rads per hour, were directed upward through a well in the lead shielding. The sample holder consisted of a pyrex cup into which was placed a thin aluminum plate. The samples were placed on the plate, and a gold-plated copper block was placed on the samples, in contact with the electrodes. The aluminum plate was then grounded, and the copper block was connected to a dry cell through a potentiostat, allowing the gate oxide to be biased to +20 volts. The pyrex cup was then lowered into the well, and the source activated while the chamber was flushed with nitrogen.

G. Capacitance-Voltage Characteristics

Flat-band voltage shifts in capacitance-voltage curves were used to determine oxide charge in MOS devices. Experimentally, a dc ramp generator was connected to a gold-plated probe through a Boonton Model 71A capacitance meter, which superimposes upon the varying dc bias a one MHz ac signal and measures the small-signal (15 mV) capacitance. The device was placed on a gold-plated stage, which was grounded, and the probe was brought into contact with the aluminum dot. A second probe was connected to the negative terminal of a 45 volt dry cell and brought into contact with the guard-ring. The gate electrode bias voltage was scanned at the rate of approximately 1 V/sec from negative to positive voltages with

a variable voltage power supply, and the C-V curve recorded on a Houston Instruments x-y recorder.

H. Bias-Temperature Stress Measurements

In order to perform bias-temperature stress measurements on MOS samples a new apparatus was designed. A stainless steel pedestal was constructed which could be electrically grounded, and which was heated by two cartridge heaters (Hotwatt, Inc., Danvers, Massachusetts) imbedded in the pedestal base. A gold-plated probe, which could be brought into contact with the aluminum gate electrode, was connected to a dry cell through a potentiostat, and was used to control the bias placed on the sample. Pedestal temperature was measured by a Honeywell DC 100B differential voltmeter, through a chromel-alumel thermocouple. After holding the sample at +20 V bias, 300°C for fifteen minutes in a nitrogen stream, the heaters were turned off, and the samples were cooled to room temperature under bias, in a stream of air from a Dyna-Vac Model 4K air pump.

4. EXPERIMENTAL RESULTS AND DISCUSSION

A. SiO_2 Etch Rate Studies

In order to determine impurity concentration profiles in silicon dioxide films by analysis of etching solutions the exact etch rate in 5% hydrofluoric acid must be determined. A series of oxides approximately 2000 Å thick was prepared. All oxides were ^{22}Na-doped, and were then subjected to various combinations of aluminum diffusion and γ-irradiation, as listed in Table 1. The oxide capacitance, C_{ox}, was measured using the capacitance-voltage technique, and this quantity was converted to oxide thickness (2):

$$x_o = \frac{\varepsilon\varepsilon_o A}{C_{ox}} \qquad (12)$$

The electrodes were removed in PAN etch, and the oxides were etched at room temperature in 5% hydrofluoric acid for two minutes, after which x_o was again determined.

The results of this experiment are given in Table 1. The average etch rate of 320 Å/min. does not vary with aluminum doping or γ-irradiation.

Table 1. Effect of 500°C aluminum-diffusion, and 10^6 rad ^{60}Co γ-irradiation, on etch rate of ^{22}Na-doped SiO_2 films

Sample Treatment	Initial x_o	Final	Etch Rate, Å/min
Untreated	1990	1350	320
Al-doped (60 min)	2005	1360	323
Irradiated	1995	1360	318
Al-doped (60 min) Irradiated	1970	1330	320

B. Sodium Concentration Profiles

Oxide films doped with ^{22}Na at 500°C for two hours were found to contain 2.9×10^{10} atoms of ^{22}Na per cm^2, ± 20%. The ^{22}Na was distributed in the typical U-shaped profile shown in Fig. 9. Dilution ratios determined from surface and interface slopes and ^{22}Na concentrations were 88 and 78,respectively. The value of 88 was employed in all subsequent work. All sodium concentration profiles shown in the remainder of this chapter are the result of averaging the profiles of three samples which underwent identical treatment. The standard deviation of the data is 20%.

C. Aluminum Diffusion

A series of 2000 Å oxides was covered with aluminum and annealed at 500°C in nitrogen for time periods between fifteen minutes and two hours. The results are shown in Figs. 10 and 11.

Fig. 10 shows aluminum profiles determined by ion microprobe analysis for samples which were annealed for 15, 30 and 60 minutes. A significant increase in concentration is apparent between 30 and 60 minutes. The intermediate values after 15 minutes are unexplained at this time. A rapid decrease near the oxide surface is followed by a more gradual decrease as the $Si-SiO_2$ interface is approached. No increase in concentration near the interface is observed, but it is apparent that a significant amount of aluminum has been transported into the oxide and to the interface.

Fig. 11 illustrates the aluminum profile, determined fluorometrically, after two hours of drive-in at 500°C. Again, a

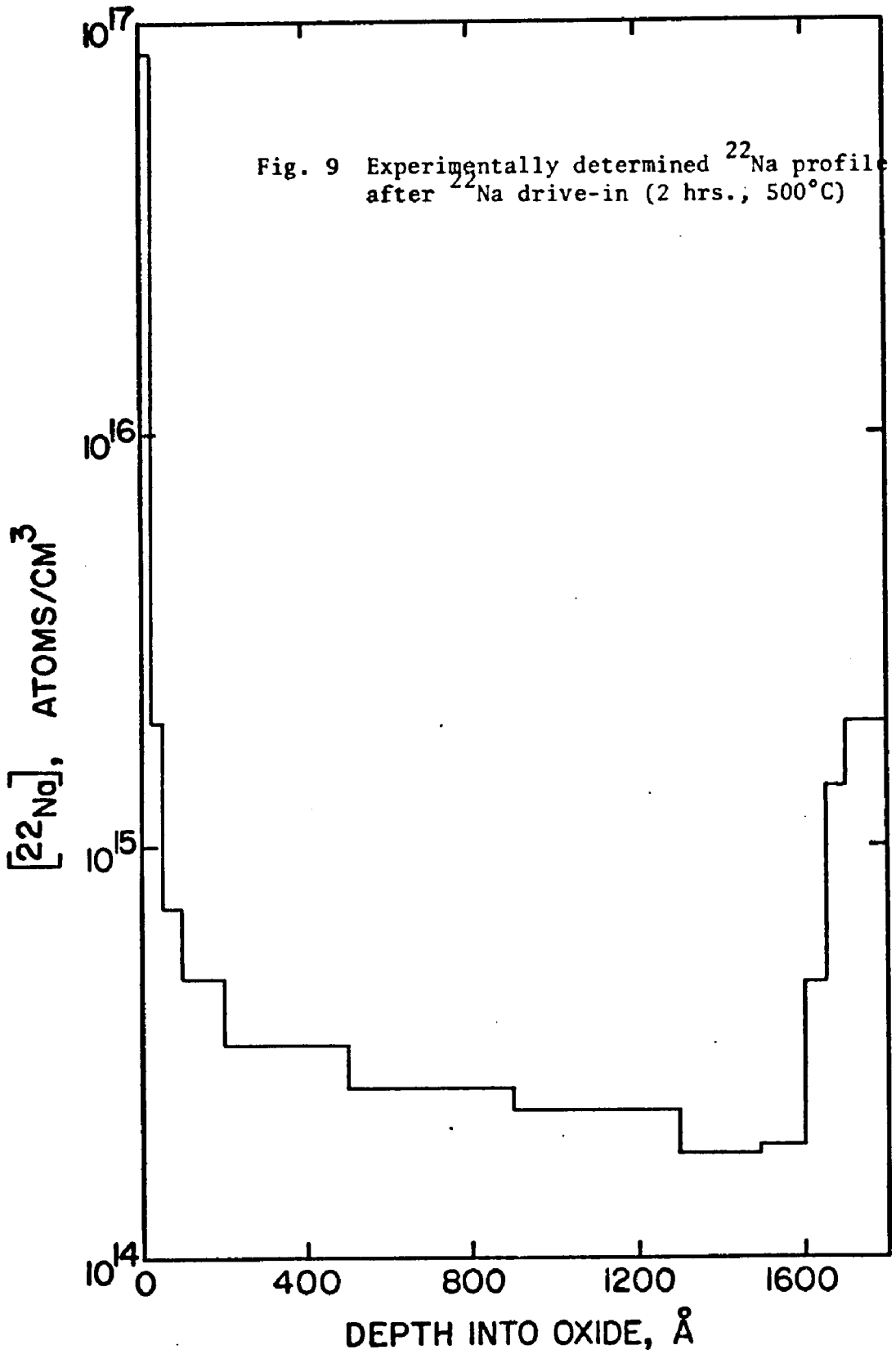

Fig. 9 Experimentally determined ^{22}Na profile after ^{22}Na drive-in (2 hrs., 500°C)

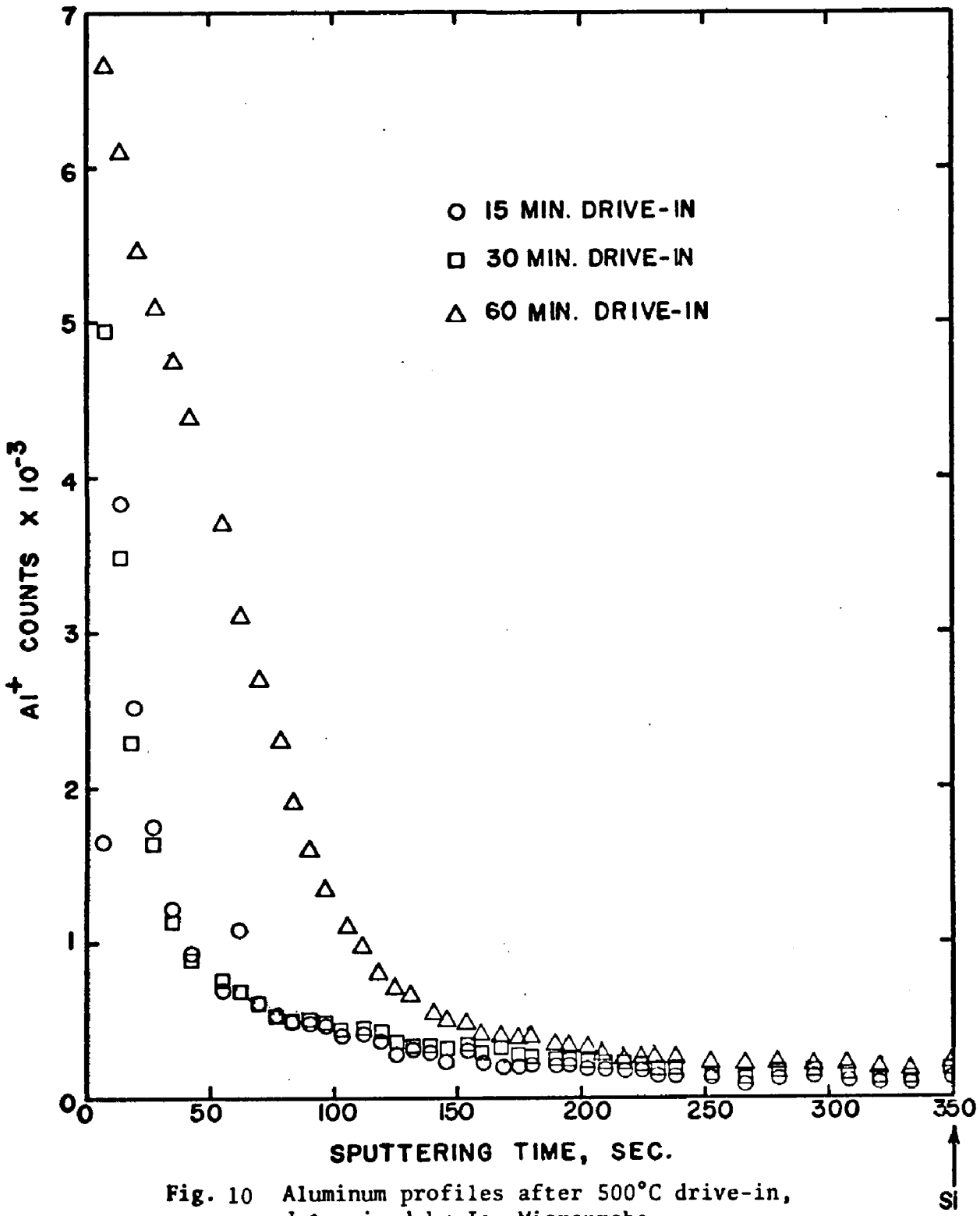

Fig. 10 Aluminum profiles after 500°C drive-in, determined by Ion Microprobe

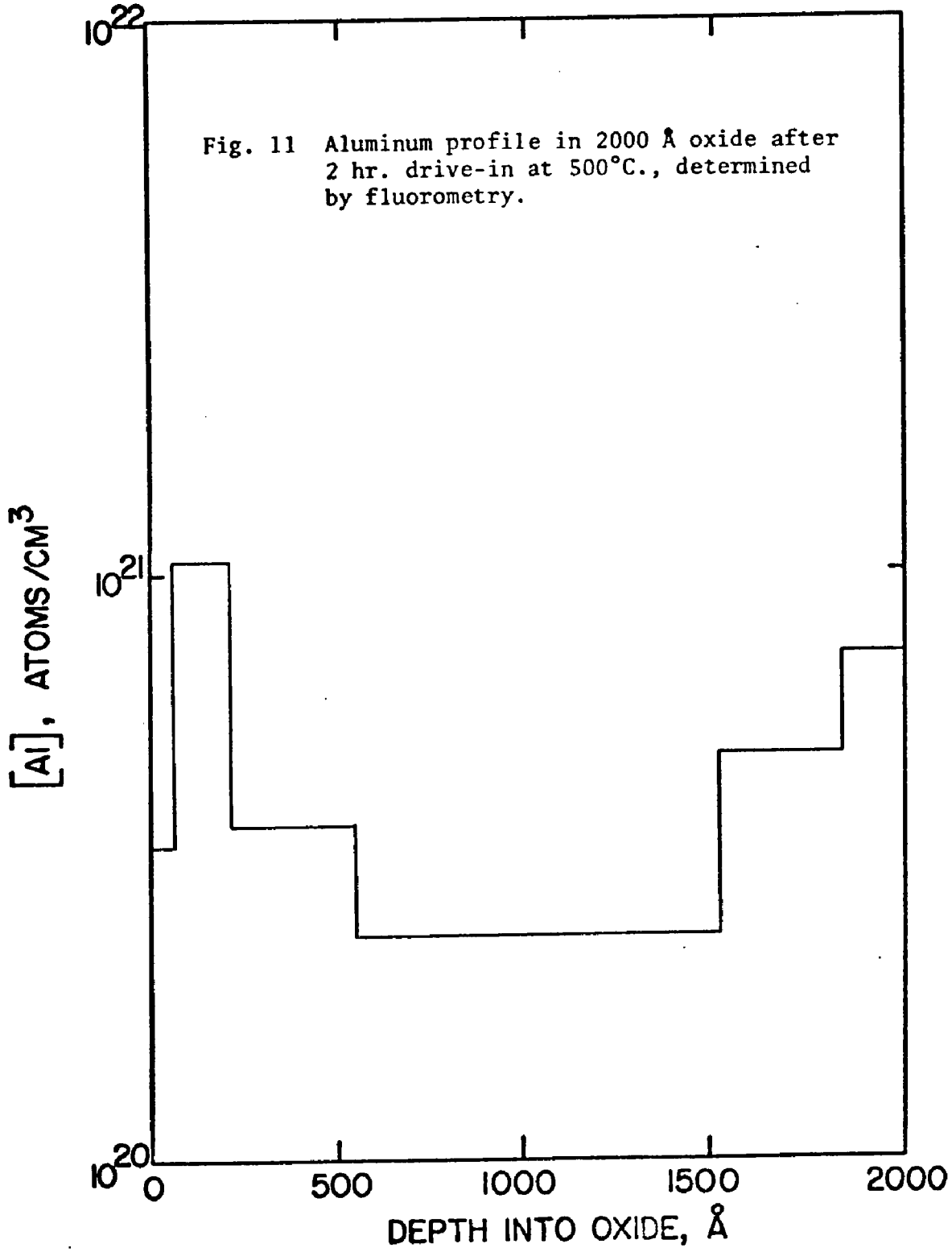

Fig. 11 Aluminum profile in 2000 Å oxide after 2 hr. drive-in at 500°C., determined by fluorometry.

considerable amount of aluminum has been driven into the oxide, and the profile is now U-shaped. The differences between the profiles shown in Figs. 10 and 11 could be explained by the longer diffusion time. Another possible explanation lies in the non-uniformity of ion etching as compared to chemical etching. Thus, if the oxide is etched to the interface in one region of the sample, but not in other regions, a flattened-out profile would be expected.

D. Capacitance-Voltage Characteristics

Capacitance-voltage characteristics were recorded, and oxide charge calculated, by the methods described in Ch. 3. The data exhibited considerable scatter, with a standard deviation of 60%. All values of oxide charge, Q_{ox}/q, are average values from three samples which underwent identical treatment.

E. Effect of Aluminum Diffusion on Oxide Charge and Sodium Profiles

Figs. 12 and 13 illustrate the effects of thirty and sixty minute aluminum diffusions on oxide charge and interfacial sodium concentrations in 1800 Å oxide films. The results are summarized in Table 2. In Fig. 12, the shifts in capacitance-voltage curves indicate a decrease in oxide charge with increasing aluminum content. MOS devices fabricated with aluminum oxide as the insulator frequently exhibit electron injection from the silicon (30). Also, aluminum-doped silicon dioxide is an acidic (electron-accepting) cracking catalyst. Thus a decrease in charge upon aluminum-doping is not surprising.

Fig. 12 Capacitance-voltage curves for aluminum-doped SiO_2 films. See Table 2.

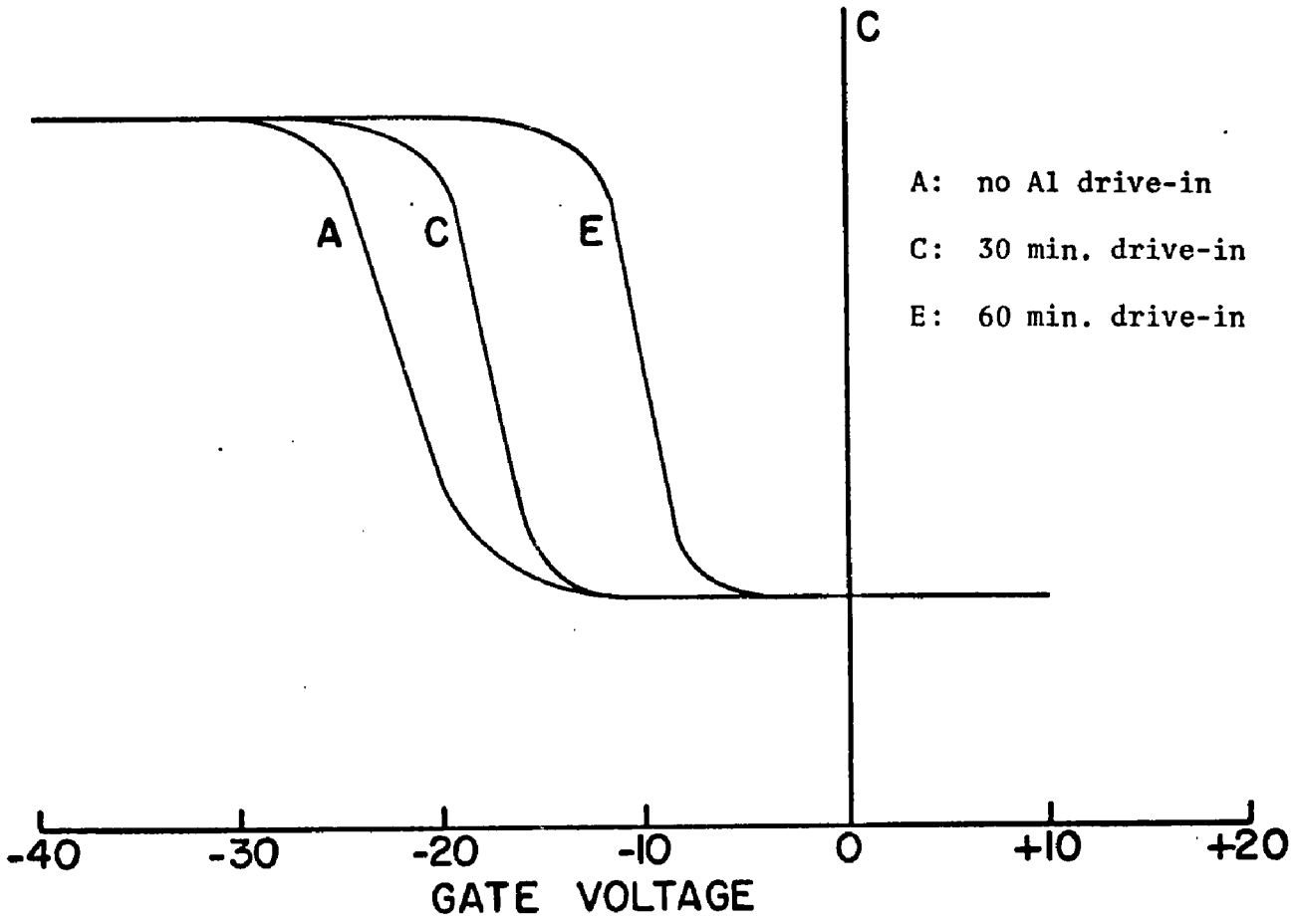

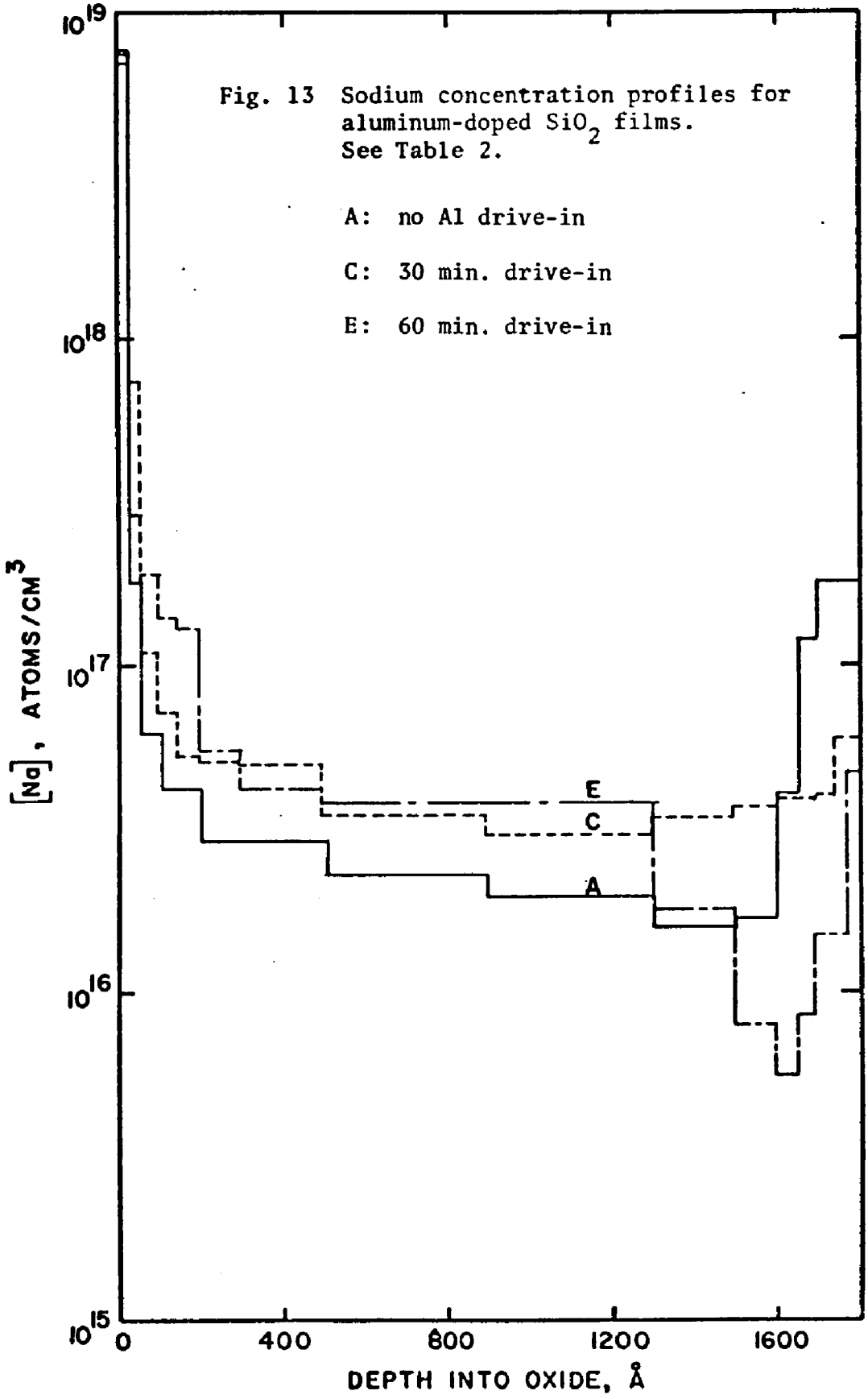

Fig. 13 Sodium concentration profiles for aluminum-doped SiO_2 films. See Table 2.

A: no Al drive-in

C: 30 min. drive-in

E: 60 min. drive-in

Table 2. Effect of 500°C aluminum diffusion on oxide charge and sodium profiles of SiO_2 films.

Sample	Treatment	$\frac{Q_{ox}}{q} \times 10^{-11}$, cm^{-2}	$[Na^+] \times 10^{-11}$, cm^{-2}			
			Surface	Bulk	Interface	Total
A	Untreated	18.9	19.7	2.7	2.4	24.8
C	Al-doped, 30 min	10.2	22.2	1.8	0.2	24.2
E	Al-doped, 60 min	5.3	24.1	1.0	0.3	25.4

Fig. 13 reveals a shift in the sodium concentration profile away from the interface, resulting in a decreased interfacial sodium concentration and an increased surface concentration. It would appear that aluminum in silicon dioxide acts as a sequestering agent for sodium, causing it to move toward those areas where the aluminum concentration is highest. The ability of aluminum to extract sodium cations from non-bridging oxygen sites in fused silica has already been suggested by the work of Sigel (10), as previously discussed in Ch. 2. The slight increase in interfacial sodium after sixty minutes of aluminum diffusion might reflect the increased interfacial aluminum content.

It is apparent that in all cases the interfacial sodium concentration constitutes only a small fraction (<10%) of the total oxide charge measured from the flat-band shift. This is especially true of those samples which have undergone thirty minute aluminum diffusions. The contribution of sodium to the oxide charge is quite small, compared to the fixed charge contribution.

F. Effect of γ-irradiation on Oxide Charge and Sodium Profiles

A series of samples was prepared and irradiated with ^{60}Co γ-irradiation (1.25 MeV) at room temperature to a dose of 10^6 rads in one hour. A gate voltage of +20 volts was applied during irradiation. The effect of such treatment is shown in Figs. 14-17 and is summarized in Table 3.

As expected, all samples exhibit an increase in oxide

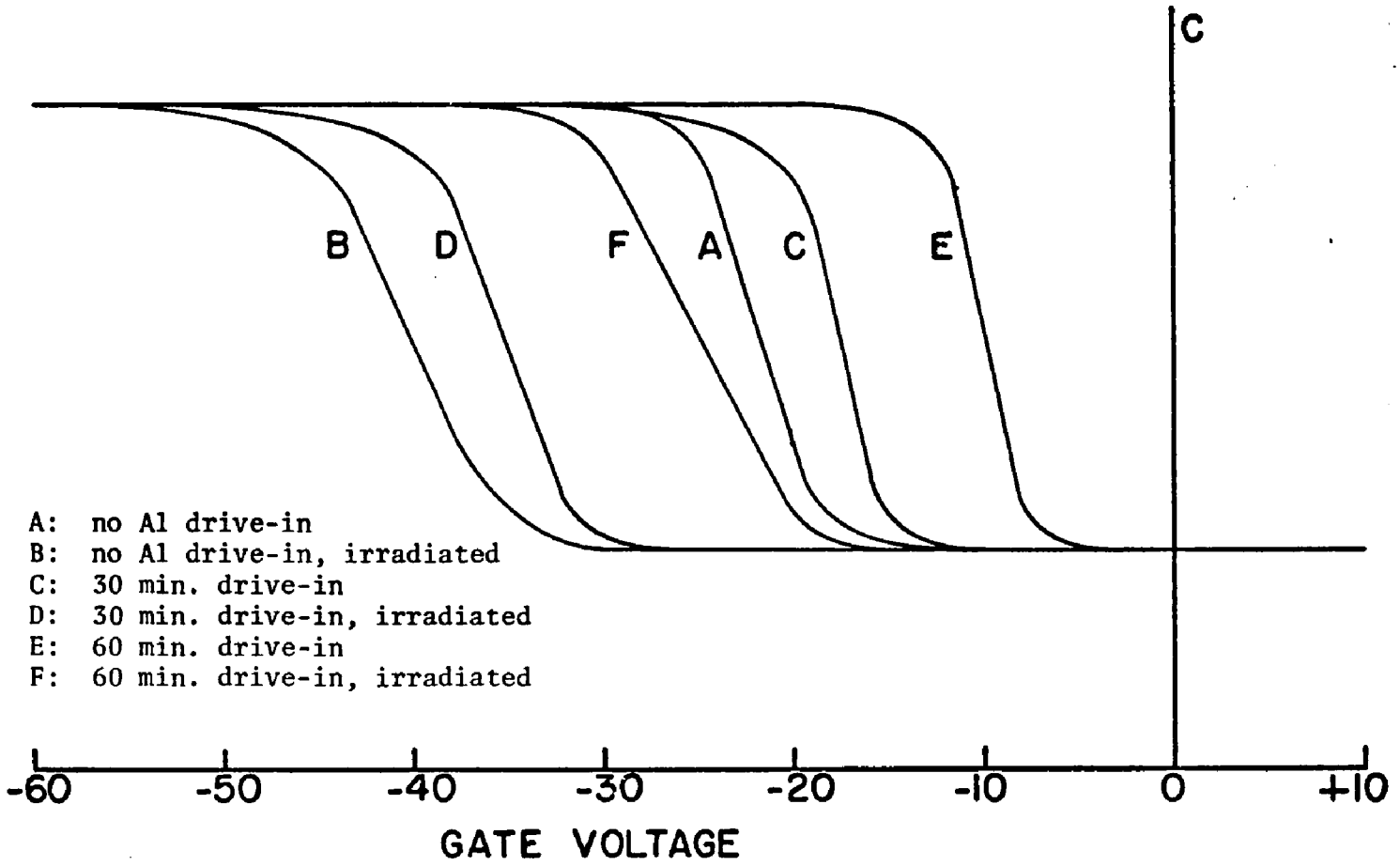

Fig. 14 Capacitance-voltage curves for γ-irradiated SiO_2 films. See Table 3.

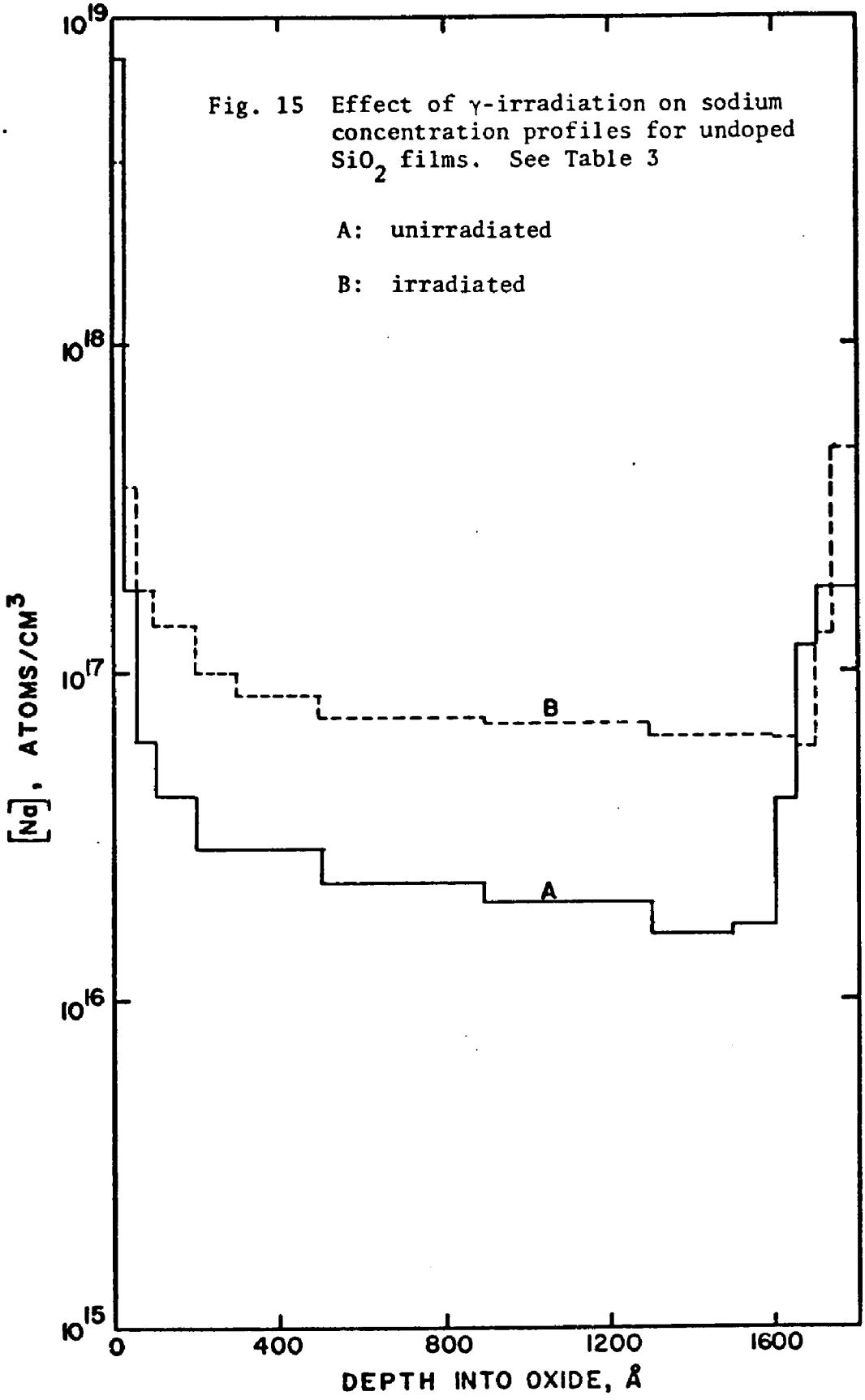

Fig. 15 Effect of γ-irradiation on sodium concentration profiles for undoped SiO_2 films. See Table 3

A: unirradiated

B: irradiated

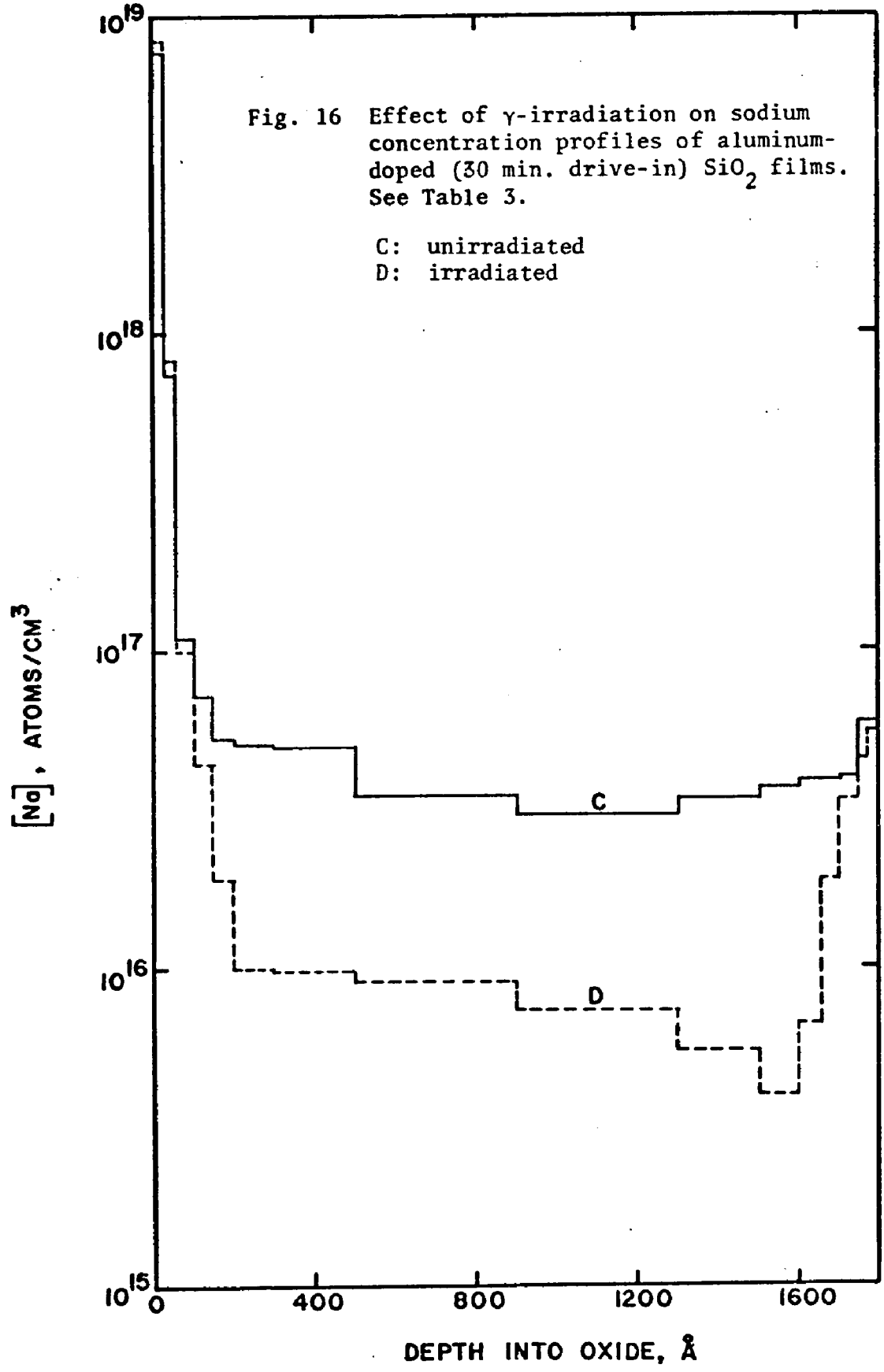

Fig. 16 Effect of γ-irradiation on sodium concentration profiles of aluminum-doped (30 min. drive-in) SiO_2 films. See Table 3.

C: unirradiated
D: irradiated

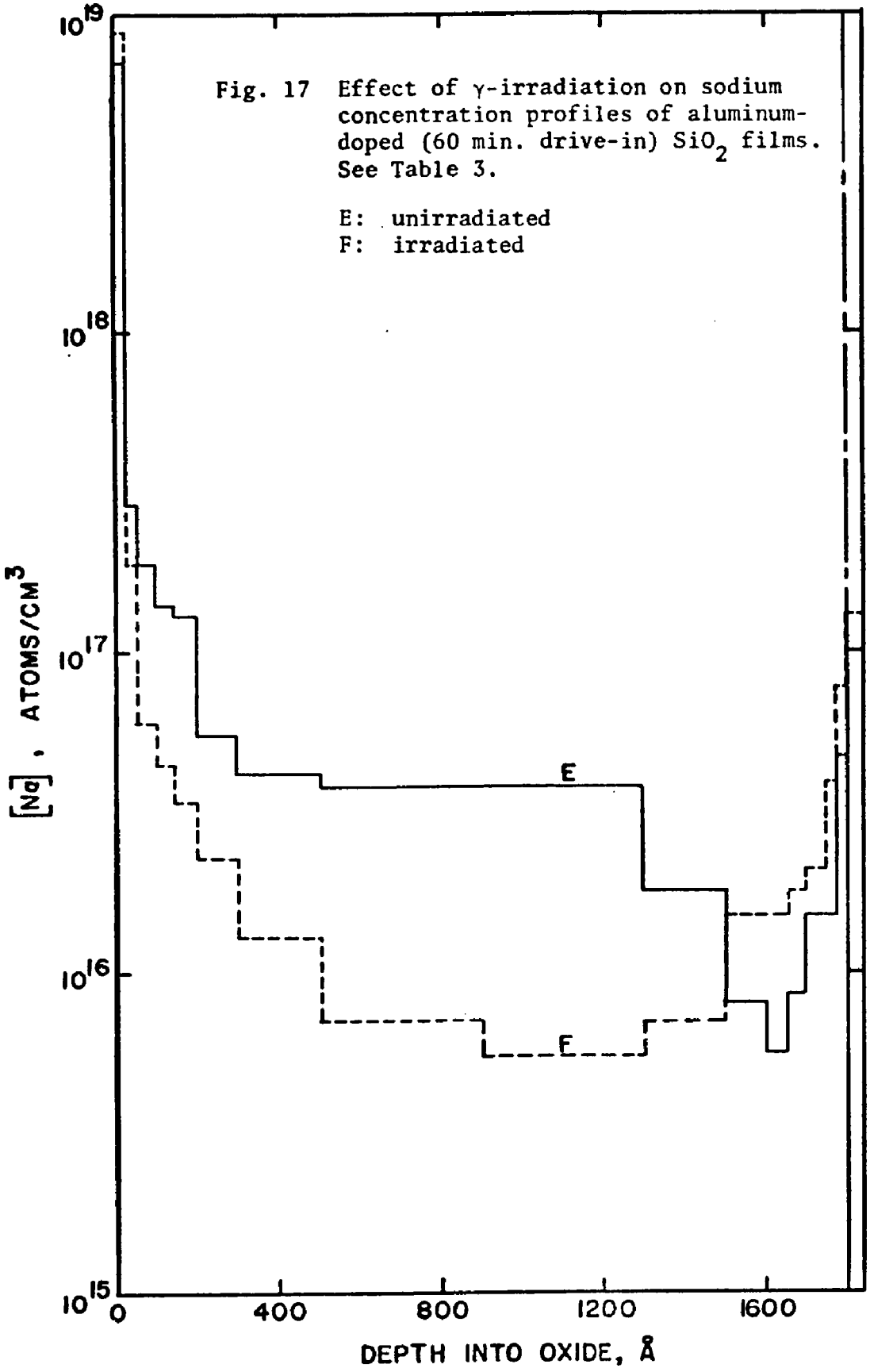

Fig. 17 Effect of γ-irradiation on sodium concentration profiles of aluminum-doped (60 min. drive-in) SiO_2 films. See Table 3.

E: unirradiated
F: irradiated

Table 3. Effect of γ-irradiation (10^6 rads, 1 hr., V_G = + 20 V) on oxide charge and sodium profiles of SiO_2 films

Sample	Treatment	$\frac{Q_{ox}}{q}$ x 10^{-11}, cm^{-2}	$[Na^+]$ x 10^{-11}, cm^{-2}			
			Surface	Bulk	Interface	Total
A	Untreated	18.9	19.7	2.7	2.4	24.8
B	Irradiated	33.5	12.3	10.2	2.6	25.1
C	Al-doped, 30 min	10.2	22.2	1.8	0.2	24.2
D	Al-doped, 30 min irradiated	29.4	24.3	0.7	0.5	25.5
E	Al-doped, 60 min	5.3	24.1	1.0	0.3	25.4
F	Al-doped, 60 min, irradiated	22.5	23.5	0.8	1.2	25.5

charge after irradiation. However, the charge in aluminum-doped oxides remains lower than that in undoped samples, and decreases with increasing aluminum content.

The interfacial sodium content, however, changes in an altogether different manner. In the undoped oxides, Fig. 15, there is a significant shift in the sodium profile away from the oxide surface, increasing the content of the central portion of the film. Although the interfacial concentration has not increased significantly, its distribution has narrowed, and the fraction immediately adjacent to the interface has increased. This result indicates that although some sodium is freed by γ-irradiation, its room temperature mobility is not drastically increased by such treatments.

Aluminum-doped samples exhibit a small increase in interfacial sodium concentration after γ-irradiation, as illustrated in Figs. 16 and 17. As with unirradiated samples, the interfacial sodium content of the more highly doped oxides is greater than that of oxides with less aluminum. The interfacial build-up is primarily at the expense of the central portions of the oxide, whose sodium concentrations have dropped considerably. It is in this region that the aluminum content of the films is lowest, so that most of the sodium is likely to be trapped at non-bridging oxygen sites. If this sodium is freed by radiation-induced hole capture, it apparently is sequestered by the interfacial aluminum. This effect

is most noticeable in the more highly aluminum-doped oxides.

G. Effect of Positive Bias-Temperature Stress on Unirradiated Oxides

Undoped oxides and oxides with two different levels of aluminum doping were subjected to bias-temperature stress at 300°C for fifteen minutes under a gate bias of +20 volts. Capacitance-voltage curves before and after such treatments are shown in Fig. 18, while Figs. 19-21 illustrate the effects of this treatment on sodium profiles. The results are summarized in Table 4.

In the undoped oxide PBT stress produces no increase in oxide charge within experimental error, while aluminum-doped samples exhibit large increases in charge, an indication that these oxides contain a considerable amount of mobile ionic charge. In fact, the oxide charge increases with increasing aluminum content, suggesting the presence of mobile interstitial aluminum.

Examination of the corresponding sodium profiles reveals modest increases in interfacial sodium concentrations in the undoped and lightly alumunum-doped oxides, while the heavily aluminum-doped oxide exhibits a ten-fold increase in interfacial sodium. The increase is almost exclusively at the expense of the sodium in the center of the film. These results indicate that although moderate aluminum doping tends to limit the mobility of sodium under PBT stress, heavy aluminum doping actually increases sodium mobility under these conditions, probably due to the large

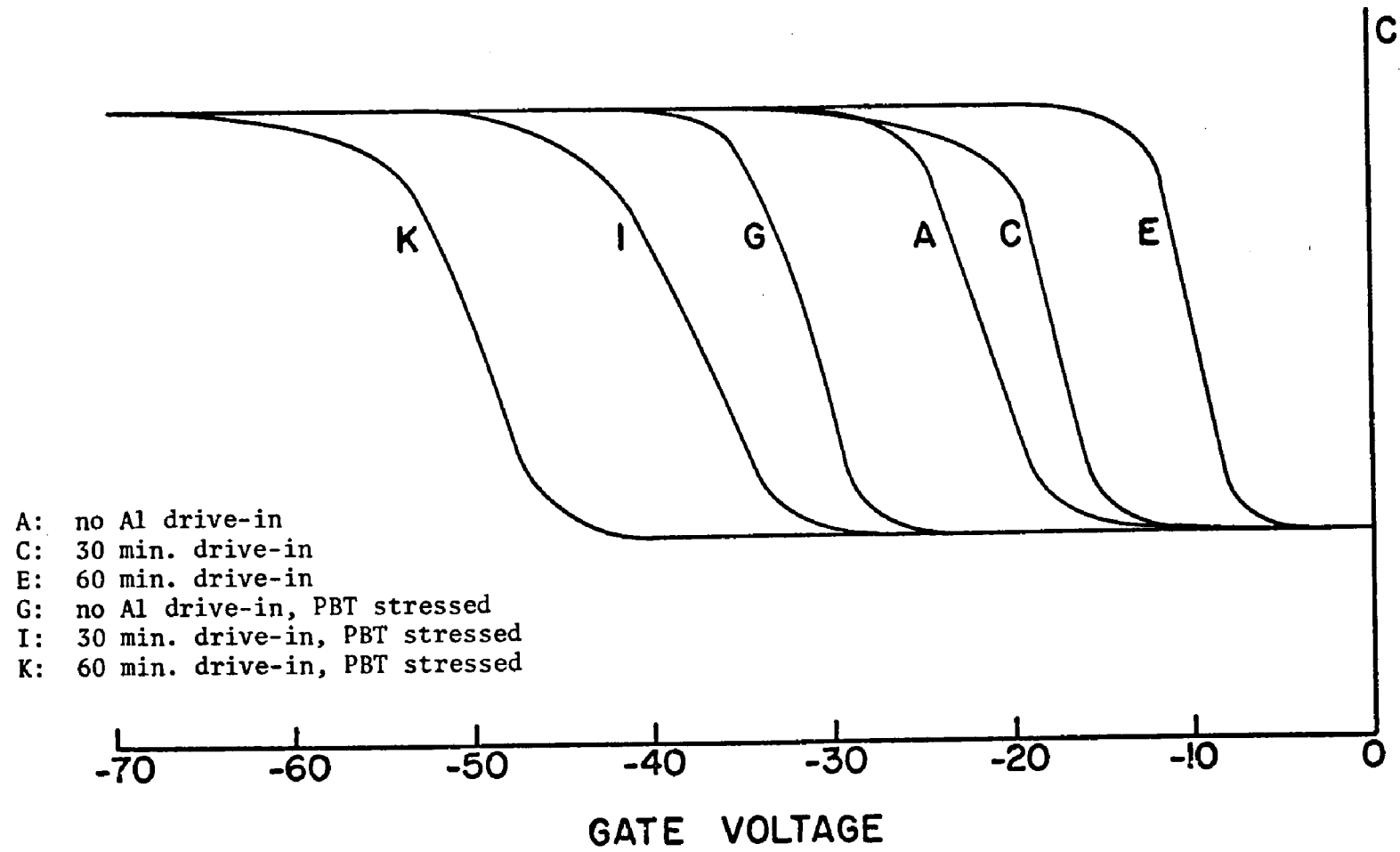

Fig. 18 Capacitance-voltage curves for SiO_2 films after positive bias-temperature stress. See Table 4.

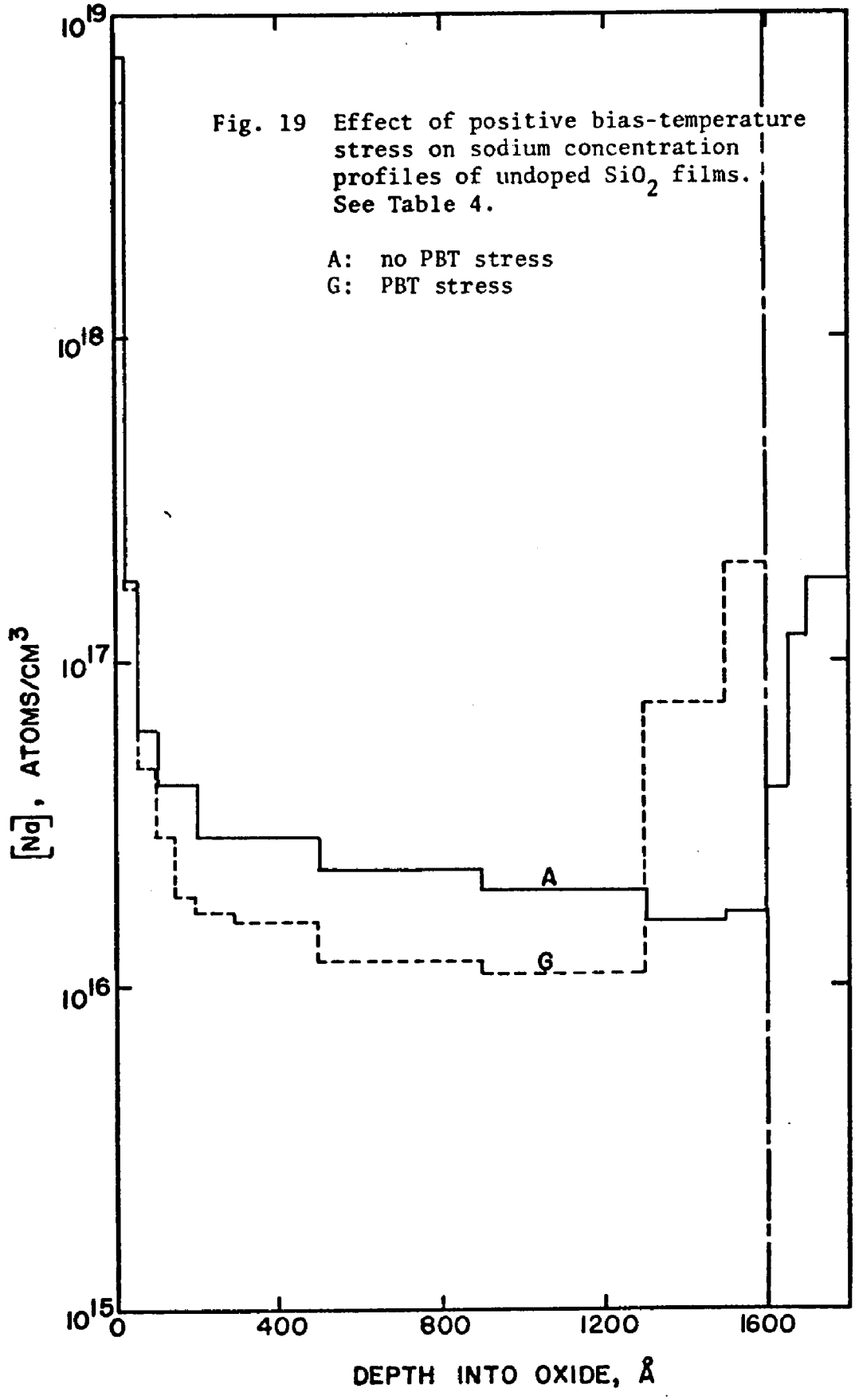

Fig. 19 Effect of positive bias-temperature stress on sodium concentration profiles of undoped SiO_2 films. See Table 4.

A: no PBT stress
G: PBT stress

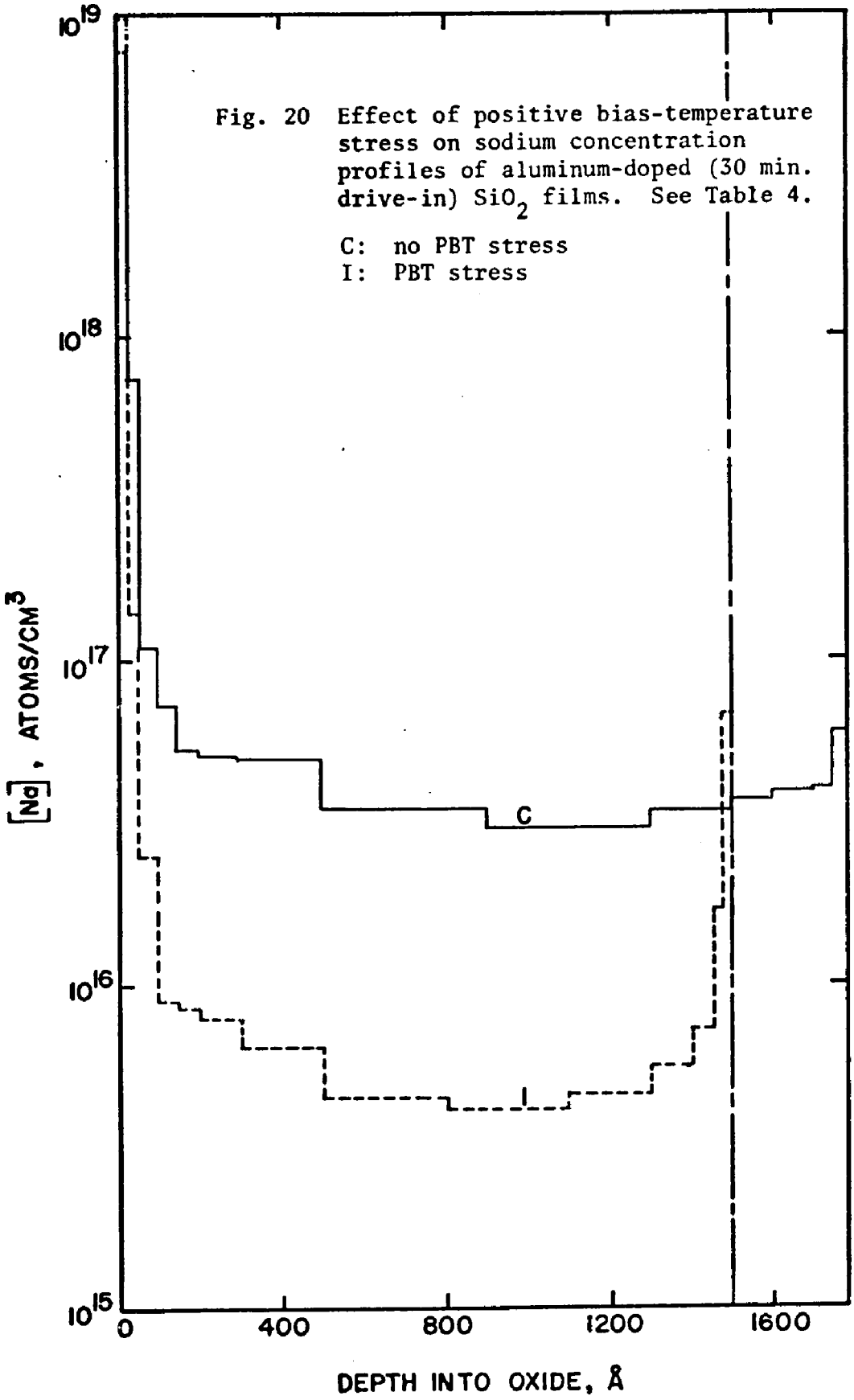

Fig. 20 Effect of positive bias-temperature stress on sodium concentration profiles of aluminum-doped (30 min. drive-in) SiO_2 films. See Table 4.

C: no PBT stress
I: PBT stress

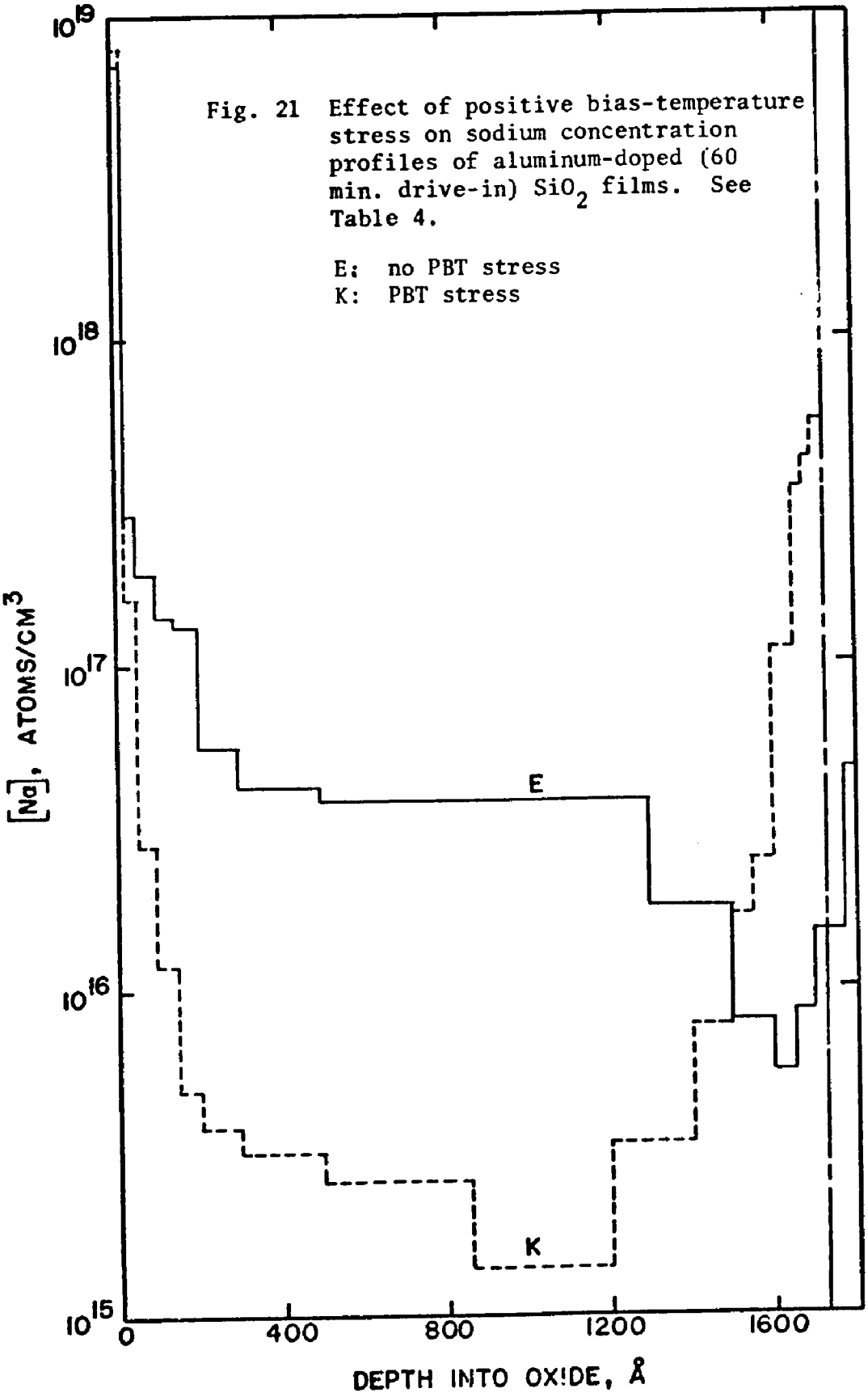

Fig. 21 Effect of positive bias-temperature stress on sodium concentration profiles of aluminum-doped (60 min. drive-in) SiO_2 films. See Table 4.

E: no PBT stress
K: PBT stress

Table 4. Effect of positive bias-temperature stress (300°C, 15 min., V_G = + 20 V) on oxide charge and sodium profiles of SiO_2 films

Sample	Treatment	$\frac{Q_{ox}}{q} \times 10^{-11}$, cm^{-2}	$[Na^+] \times 10^{-11}$, cm^{-2}			
			Surface	Bulk	Interface	Total
A	Untreated	18.9	19.7	2.7	2.4	24.8
G	PBT stressed	24.0	14.4	1.9	3.5	19.8
C	Al-doped, 30 min	10.2	22.2	1.8	0.2	24.2
I	Al-doped, 30 min, PBT stressed	25.5	24.6	0.7	0.4	25.7
E	Al-doped, 60 min	5.3	24.1	1.0	0.3	25.4
K	Al-doped, 60 min PBT stressed	32.0	20.6	0.2	3.2	24.0

number of sodium trapping sites in the highly-aluminum-doped interfacial region.

H. Effect of Positive Bias-Temperature Stress on Irradiated Oxides

The ability of γ-irradiation to liberate mobile charge was studied by subjecting previously irradiated oxides (10^6 rad, +20V gate bias, one hour) to PBT stress (300°C, +20V gate bias, fifteen minutes). The results are illustrated in Figs. 22-25 and summarized in Table 5.

It is apparent from Fig. 22 and Table 5 that irradiation liberates charge which is not mobile at room temperature, but which can be made to drift at elevated temperatures. The largest amount of liberated charge occurs in the oxide with the highest aluminum content.

The build-up in interfacial sodium content upon PBT stress of irradiated oxides is quite pronounced in the undoped and heavily aluminum-doped oxides. The build-up is at the expense of sodium in the center of the film. By contrast, there is comparatively little change in the interfacial sodium content of the moderately aluminum-doped oxide.

It would appear that, as indicated in the previous section, moderate aluminum concentrations are beneficial in reducing oxide charge and sodium mobility, while heavily doped oxides are somewhat less stable.

Fig. 22 Capacitance-voltage curves for γ-irradiated SiO_2 films after subsequent positive bias-temperature stress. See Table 5.

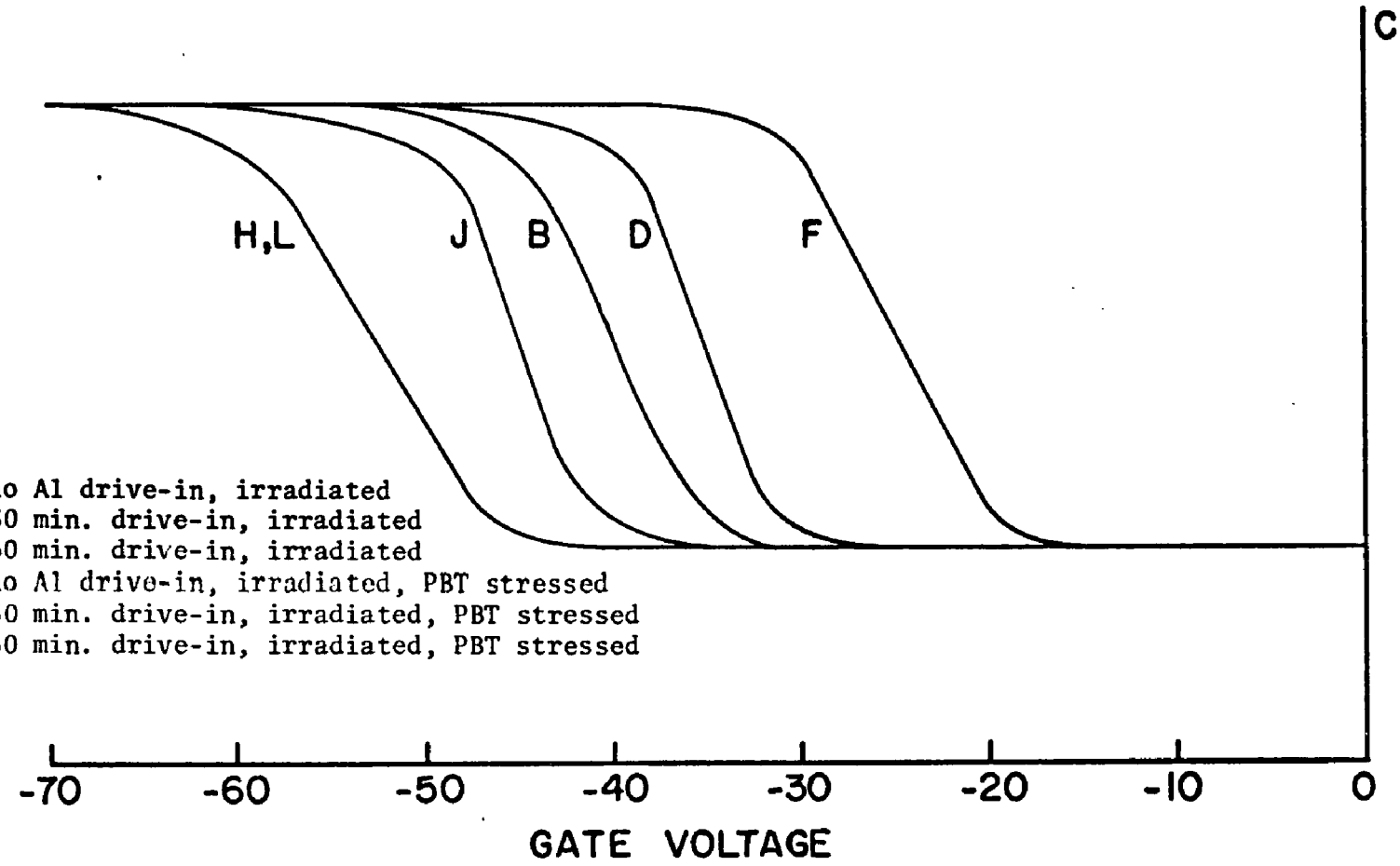

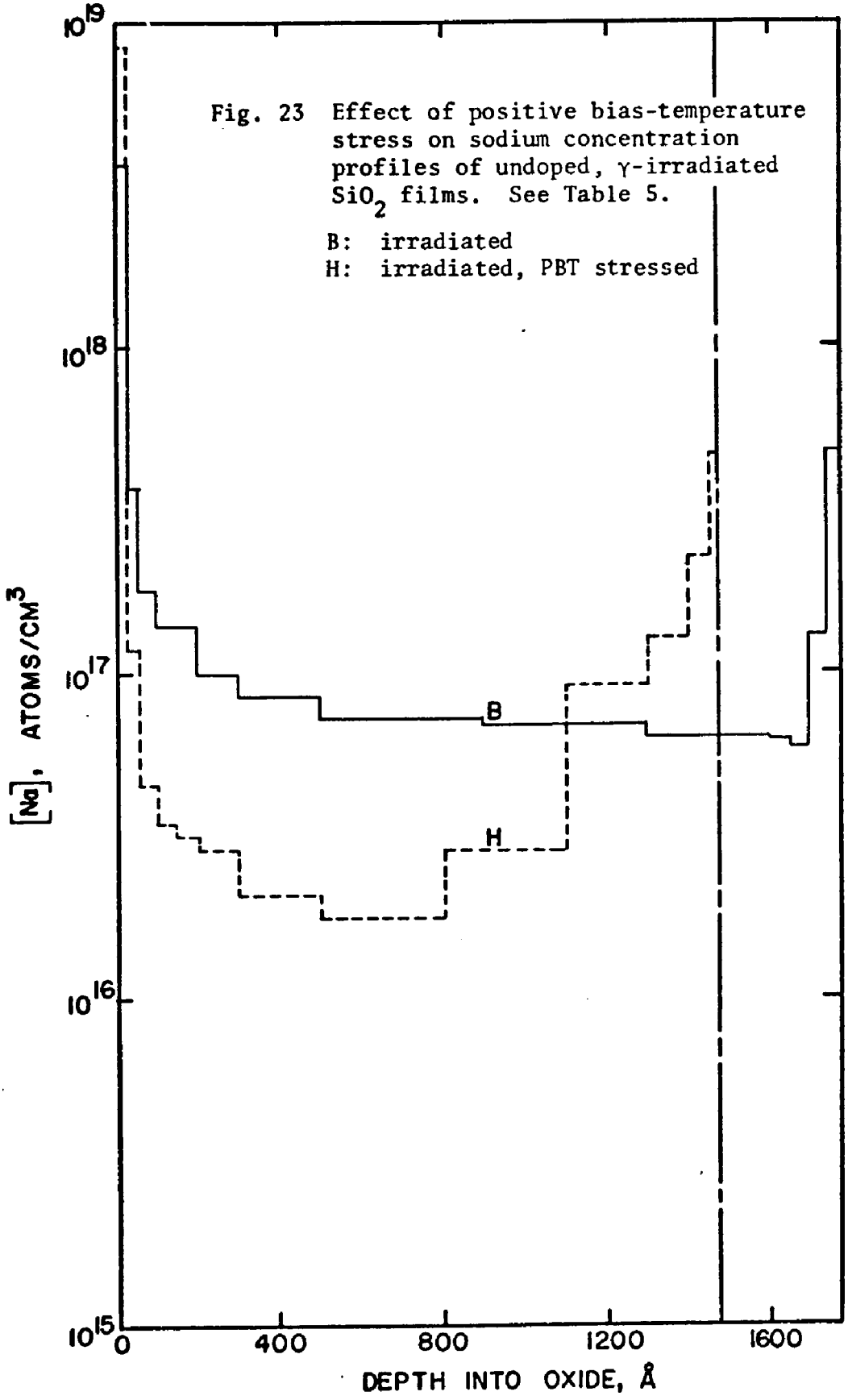

Fig. 23 Effect of positive bias-temperature stress on sodium concentration profiles of undoped, γ-irradiated SiO_2 films. See Table 5.

B: irradiated
H: irradiated, PBT stressed

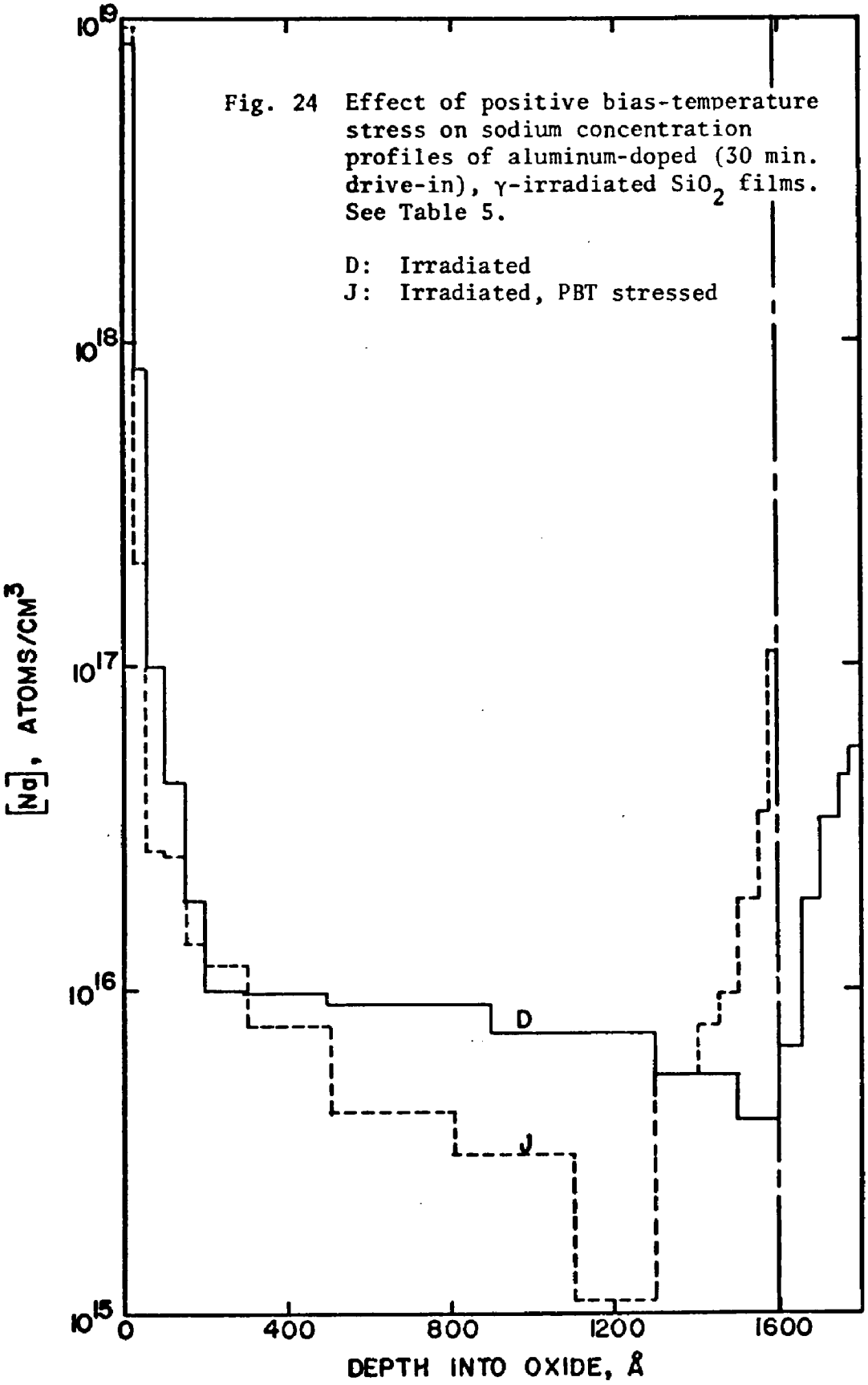

Fig. 24 Effect of positive bias-temperature stress on sodium concentration profiles of aluminum-doped (30 min. drive-in), γ-irradiated SiO_2 films. See Table 5.

D: Irradiated
J: Irradiated, PBT stressed

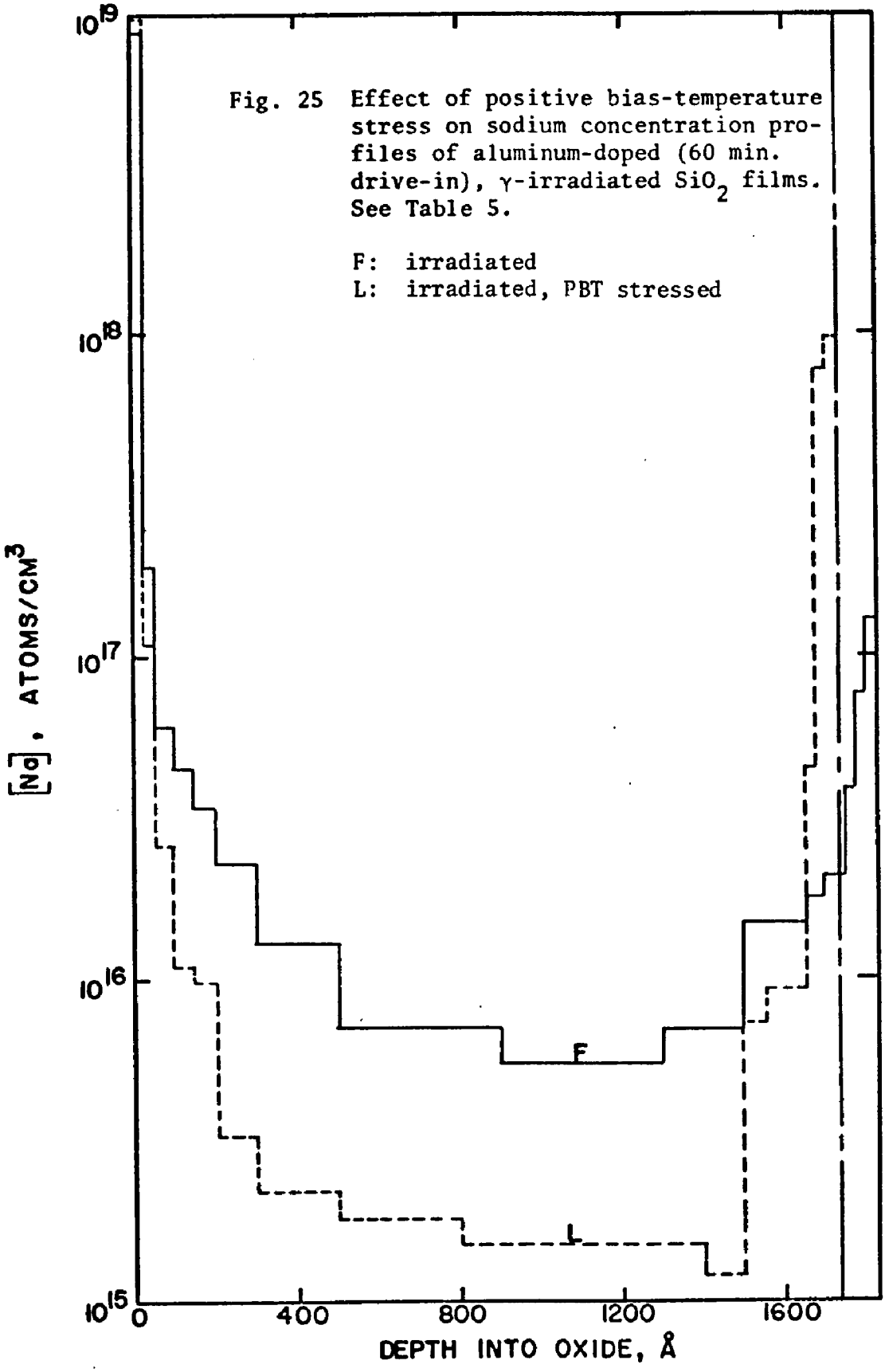

Fig. 25 Effect of positive bias-temperature stress on sodium concentration profiles of aluminum-doped (60 min. drive-in), γ-irradiated SiO_2 films. See Table 5.

F: irradiated
L: irradiated, PBT stressed

Table 5. Effect of positive bias-temperature stress (300°C, + 20 V, 15 min.) on oxide charge and sodium profiles of γ-irradiated SiO_2 films.

Sample	Treatment	$\frac{Q_{ox}}{q} \times 10^{-11}$, cm^{-2}	$[Na^+] \times 10^{-11}$, cm^{-2}			
			Surface	Bulk	Interface	Total
B	Irradiated	33.5	12.3	10.2	2.6	25.1
H	Irradiated, PBT stressed	44.4	21.8	3.0	6.3	31.1
D	Al-doped, 30 min, irradiated	29.4	24.3	0.7	0.5	25.5
J	Al-doped, 30 min, irradiated, PBT stressed	36.1	24.7	0.2	0.6	25.5
F	Al-doped, 60 min, irradiated	22.5	23.5	0.8	1.2	25.5
L	Al-doped, 60 min, irradiated, PBT stressed	45.3	24.8	0.2	4.6	29.6

5. SUMMARY AND CONCLUSIONS

1. A study has been made of the effect of γ-irradiation and aluminum doping on oxide charge and sodium mobility in thermally grown silicon dioxide films on silicon.

2. Sodium-22 can be diffused into the films at 500°C. After two hours the ^{22}Na has assumed a U-shaped concentration profile. The slope of this profile at the silicon dioxide surface, or at the $Si-SiO_2$ interface, can be used to determine the total sodium concentration profile in the oxide.

3. Aluminum can be diffused through a 2000 Å silicon dioxide film in thirty minutes. Diffusion for longer times increases the aluminum content of the films near the $Si-SiO_2$ interface.

4. Interfacial sodium impurities account for only a small portion (<10%) of the total oxide charge measured by flat-band shifts in capacitance-voltage curves of MOS capacitors. This result indicates that other charged species, such as ionized oxygen vacancies (17), contribute oxide charge.

5. Moderate aluminum diffusion causes a shift of the sodium concentration profile toward the oxide surface, lowering the interfacial sodium concentration. Heavy aluminum doping, which results in an interfacial aluminum build-up, also results in a build-up at the surface. This apparent sequestering ability of aluminum for sodium occurs at the expense of the sodium content in the center of the film.

10^6 rads of ^{60}Co γ-radiation under positive gate bias causes an increase in oxide charge. Although the charge after irradiation decreases with increasing aluminum doping, the difference in the charge between unirradiated and irradiated films increases with increasing aluminum content. The oxygen vacancy content of the films should increase with the substitutional aluminum content. These vacancies can act as hole traps during irradiation:

$$V_o + h^+ \rightleftharpoons V_o^+$$

Thus, they may contribute to the radiation-induced positive oxide charge. Irradiation results in a small shift in the sodium profile toward the interface in undoped oxides, and an increased interfacial sodium content in the aluminum-doped oxides, with the heavily-doped oxide showing a larger build-up than the moderately-doped sample. Again, the build-up at the interface is accompanied by a decrease in sodium content in the center of the film.

7. PBT stress (300°C, +20 volts gate bias, fifteen minutes) of unirradiated samples results in an increase in oxide charge only in aluminum doped samples. The charge increases with increasing aluminum content. Interfacial sodium concentrations also increase after PBT stress, with undoped and heavily doped oxides exhibiting similar values, while the moderately doped samples are much lower.

8. PBT stress of irradiated oxides results in increased oxide charge in all samples. Increases in interfacial sodium at the expense of sodium in the bulk are also observed in the undoped and heavily aluminum-doped oxides.

9. These results are consistent with a model in which sodium cations, initially trapped at sites which have been suggested to be non-bridging oxygen ions (9,10,27), are extracted from these sites by negatively-charged substitutional aluminum centers. Such a process has been postulated in bulk silica by Sigel (10). Thus, in aluminum-doped oxides, the sodium tends to concentrate in the areas of highest aluminum concentration. Sodium may also be freed from trapping sites by radiation-induced hole capture, as suggested by Lineweaver (9), etc. This liberated sodium, which is only slightly mobile at room temperature, but which has high mobility at elevated temperatures, will tend to move toward the interface under positive gate bias unless or until it is recaptured by another aluminum center.

10. Gamma-irradiation followed by bias-temperature stress resulted in a ten-fold increase in oxide charge in the heavily-aluminum doped samples. Heavy aluminum doping may result in a large concentration of interstitial aluminum, which in turn may be sufficiently mobile to drift to the interface and increase oxide charge.

REFERENCES

1. A. S. Grove, Physics and Technology of Semiconductor Devices, John Wiley and Sons, Inc., New York, 1967.

2. S. M. Sze, Physics of Semiconductor Devices, Wiley Interscience, New York, 1969.

3. E. Lell, N. J. Kreidl, and J. R. Hensler, in Progress in Ceramic Science, ed. by J. E. Burke, Pergamon Press, Oxford, 1966, Vol. 4, p. 1.

4. R. W. Ditchburn, E. W. J. Mitchell, E. G. S. Paige, J. F. Custers, H. B. Dyer, and C. D. Clark, in Defects in Crystalline Solids: Report of the Bristol Conference, Physical Society, London, 1955, p. 92.

5. J. H. E. Griffiths, J. Owen, and I. M. Ward, in Defects in Crystalline Solids: Report of the Bristol Conference, Physical Society, London, 1955, p. 81.

6. M. C. M. O'Brien, Proc. Roy. Soc. A231, 404 (1955).

7. E. W. J. Mitchell and E. G. S. Paige, Phil. Mag. 46, 1353 (1955).

8. E. Lell, Phys. Chem. Glasses 3, 84 (1962).

9. J. L. Lineweaver, J. Appl. Phys. 34, 1786 (1963).

10. G. H. Sigel, Jr., J. Phys. Chem. Solids 32, 2373 (1971).

11. G. W. Arnold, Jr., Proc. 10th Ann. Symp. on Freq. Control, Asbury Park, N. J., Mar. 1955.

12. J. H. Mackey, Jr., J. Chem. Phys. 39, 74 (1963).

13. R. A. Weeks, J. Amer. Ceram. Soc. 53, 176 (1970).

14. A. Halperin and J. E. Ralph, J. Chem. Phys.39, 63 (1963).

15. C. E. Jones, private communication.

16. A. Goetzberger, Bell Syst. Tech. J. 45, 1097 (1966).

17. F. M. Fowkes and D. W. Hess, Appl. Phys. Lett. 22, 377 (1973).

18. F. M. Fowkes and T. E. Burgess, Surface Sci. 13, 184 (1969).

19. E. Yon, W. H. Ko, and A. B. Kuper, IEEE Trans. Elec. Dev. ED-13, 276 (1966).

20. F. M. Fowkes, T. E. Burgess, and G. Hutchins, Abstract No. 175, Electrochemical Society Meeting, Philadelphia, Oct. 1966.

21. N. J. Chou and J. M. Eldridge, J. Electrochem. Soc. 117, 1287 (1970).

22. H. M. Donega, R. L. Baker, and T. E. Burgess, Abstract No. 126, Electrochemical Society Meeting, New York, May 1969.

23. J. P. Mitchell and D. K. Wilson, Bell Syst. Tech. J. 46, 1 (1967).

24. E. H. Snow, A. S. Grove, and D. J. Fitzgerald, Proc. IEEE 55, 1168 (1967).

25. A. G. Revesz, K. H. Zaininger, and R. J. Evans, J. Electrochem. Soc. 116, 1146 (1969).

26. J. L. Peel and G. Kinoshita, IEEE Trans. Nucl. Sci. NS-19(6), 271 (1972).

27. H. L. Hughes, R. D. Baxter, and B. Philips, IEEE Trans. Nucl. Sci. NS-19 (6), 256 (1972).

28. C. W. Gwyn, J. Appl. Phys. 40, 4886 (1969).

29. F. Will, III, Anal. Chem. 33, 1361 (1961).

30. K. M. Schlesier and P. E. Norris, IEEE Trans. Nucl. Sci. NS-19(6), 275 (1972).

VITA

Frederick Everett Witherell, Jr., the son of Mary L. and Frederick E. Witherell, was born in Elizabeth, New Jersey, on August 15, 1946. He graduated from Thomas Jefferson High School in Elizabeth in June, 1964, and entered Lehigh University in the following September. Mr. Witherell received the Bachelor of Science and Master of Science degrees in Chemical Engineering from Lehigh in June, 1968, and June, 1970, respectively. After a brief tour of military service, Mr. Witherell returned to Lehigh in November, 1970, as a research assistant on a National Science Foundation grant. Since July, 1973, he has received support from the Defense Nuclear Agency.

Mr. Witherell is married to the former Marilyn A. Swingle of Bethlehem, Pennsylvania.